



1 **Review article: A systematic review of terrestrial dissolved organic carbon in northern**  
2 **permafrost**

3 Liam Heffernan<sup>1</sup>, Dolly N. Kothawala<sup>1</sup>, Lars J. Tranvik<sup>1</sup>

4

5 <sup>1</sup>Limnology/Department of Ecology and Genetics, Uppsala University, Norbyvägen 18D,  
6 Uppsala 75236, Sweden

7

8 Correspondence email: [liam.heffernan@ebc.uu.se](mailto:liam.heffernan@ebc.uu.se)

9

10

11

12

13

14

15

16

17

18

19

20

21

22



## 23 **Abstract**

24 As the permafrost region warms and permafrost soils thaw, vast pools of soil organic  
25 carbon (C) become vulnerable to enhanced microbial decomposition and lateral transport into  
26 aquatic ecosystems as dissolved organic carbon (DOC). The mobilization of permafrost soil C  
27 can drastically alter the net northern permafrost C budget. DOC entering aquatic ecosystems  
28 becomes biological available for degradation as well as other types of aquatic processing.  
29 However, it currently remains unclear which landscape characteristics are most relevant to  
30 consider in terms of predicting DOC concentrations entering aquatic systems from permafrost  
31 regions. Here, we conducted a systematic review of 111 studies relating to, or including,  
32 concentrations of DOC in terrestrial permafrost ecosystems in the northern circumpolar region  
33 published between 2000 – 2022. We present a new permafrost DOC dataset consisting of 2,276  
34 DOC concentrations, collected from the top 3 m in permafrost soils across the northern  
35 circumpolar region. Concentrations of DOC ranged from 0.1 – 500 mg L<sup>-1</sup> (median = 41 mg L<sup>-1</sup>)  
36 across all permafrost zones, ecoregions, soil types, and thermal horizons. DOC concentrations  
37 were greatest in the sporadic permafrost zone (101 mg L<sup>-1</sup>) while lower concentrations were  
38 found in the discontinuous (60 mg L<sup>-1</sup>) and continuous (59 mg L<sup>-1</sup>) permafrost zones. The highest  
39 median DOC concentrations of 66 mg L<sup>-1</sup> and 63 mg L<sup>-1</sup> were found in coastal tundra and  
40 permafrost bog ecosystems, respectively. Coastal tundra (130 mg L<sup>-1</sup>), permafrost bogs (78 mg  
41 L<sup>-1</sup>), and permafrost wetlands (57 mg L<sup>-1</sup>) had the highest DOC concentrations in the permafrost  
42 lens, representing a potentially long-term store of DOC. Other than in Yedoma ecosystems, DOC  
43 concentrations were found to increase following permafrost thaw and were highly constrained by  
44 total dissolved nitrogen concentrations. This systematic review highlights how DOC  
45 concentrations differ between organic- or mineral-rich deposits across the circumpolar  
46 permafrost region and identifies coastal tundra regions as areas of potentially important DOC  
47 mobilization. The quantity of permafrost-derived DOC exported laterally to aquatic ecosystems  
48 is an important step for predicting its vulnerability to decomposition.

49



## 50      **1. Introduction**

51            Persistent freezing temperatures since the late Pleistocene and Holocene has led to the  
52 accumulation and preservation of 1,460 – 1,600 Pg of organic carbon (C) in northern  
53 circumpolar permafrost soils (Hugelius et al., 2014; Schuur et al., 2018). However, in recent  
54 decades, there has been an amplified level of warming at high latitudes, occurring at four-times  
55 the speed of the global average (Rantanen et al., 2021). This is leading to widespread and rapid  
56 permafrost thawing. Under the high C emissions representative concentration pathway (RCP8.5),  
57 90% loss of near-surface permafrost is projected to occur by 2300, with the majority of loss  
58 occurring by 2100 (McGuire et al., 2018). Increasing temperatures and widespread thaw exposes  
59 permafrost C to heterotrophic decomposition, potentially leading to enhanced emissions of  
60 greenhouse gases to the atmosphere in the form of carbon dioxide (CO<sub>2</sub>; Schuur et al., 2021) and  
61 methane (CH<sub>4</sub>; Turetsky et al., 2020). Alternatively, previously frozen soil organic carbon may  
62 be mobilized into the aquatic network as dissolved organic carbon (DOC), the quantity and  
63 quality of which will likely depend on local and regional hydrology, and landscape  
64 characteristics (Tank et al., 2012; Vonk et al., 2015). At high latitudes (>50°N), lakes and rivers  
65 of various sizes cover 5.6% and 0.47% of the total area, respectively (Olefeldt et al., 2021), and  
66 the landscape C balance at these high latitudes is highly dependent on aquatic C processing  
67 (Vonk & Gustafsson, 2013). The increased leaching of recently thawed DOC from permafrost  
68 soils will not only increase the currently estimated 25 – 36 Tg DOC year<sup>-1</sup> exported into the  
69 freshwater system, and subsequently into the Arctic Ocean (Holmes et al., 2012; Raymond et al.,  
70 2007), but will also likely lead to enhanced greenhouse gas emissions from freshwater  
71 ecosystems (Dean et al., 2020). However, uncertainty remains as to which terrestrial ecosystems  
72 are likely to contribute the highest concentrations of laterally transported permafrost DOC and of  
73 this, which is expected to contribute the DOC most vulnerable to mineralization.

74            The contribution of mineralized permafrost C to atmospheric CO<sub>2</sub> and CH<sub>4</sub> balances, known  
75 as the permafrost C feedback (Schaefer et al., 2014), remains poorly constrained due to  
76 uncertainty of the magnitude and location of permafrost C emissions (Miner et al., 2022). The  
77 lateral transport of DOC represents a source of terrestrial C that can potentially play an important  
78 role in both terrestrial and aquatic biogeochemical cycles and is thus an important fraction of the  
79 permafrost C feedback. Warming of near surface permafrost causes widespread thawing (Camill,



80 2005; Jorgenson et al., 2006), which can lead to drastic changes in hydrology, vegetation, and  
81 soil carbon dynamics (Liljedahl et al., 2016; Pries et al., 2012; Varner et al., 2022). When  
82 permafrost is present, the lateral transport of DOC is restricted to flow paths within the unfrozen,  
83 organic rich active layer (Woo, 1986). Deepening of the seasonally thawed active layer due to top-  
84 down permafrost thaw can lead to longer flow paths for DOC, allowing for enhanced  
85 decomposition or adsorption to mineral particles, resulting in reduced DOC export (Kicklighter  
86 et al., 2013; Striegl et al., 2005). Alternatively, thermokarst formation can affect the entire soil  
87 profile, leading to surface inundation, and shifting ecological conditions and vegetation  
88 communities associated with greater DOC production (Turetsky et al., 2007). This can cause  
89 greater hydrological connectivity, resulting in increased runoff in permafrost peatlands (Connon  
90 et al., 2014) or increased connectivity to regional hydrology through thermo-erosion gullies or  
91 thaw slumps (Kokelj & Jorgenson, 2013) in tundra ecosystems. Permafrost landscape dynamics,  
92 including the mode of permafrost thaw and ecological conditions present following thaw, will  
93 play a key role in the biogeochemical and ecohydrological processes that constrain DOC  
94 mobilization, i.e., export and mineralization upon export. The freshwater DOC pool represents a  
95 mix of C derived from a variety of ecosystem types and sources, and the ecological conditions of  
96 each source will have a significant impact on the quantity and quality of this mobilized DOC.  
97 Determining the relative contribution and impact on mineralization of these DOC sources  
98 represents a potentially important step in reducing uncertainty in the permafrost climate  
99 feedback.

100 Here, we conduct a systematic review and compiled 111 studies published between 2000 –  
101 2022 on DOC concentrations in the top 3 m of terrestrial ecosystems found in the northern  
102 circumpolar permafrost region. A quantitative assessment of studies pertaining to DOC  
103 concentrations in permafrost soils can identify evidence-based recommendations for future topics  
104 and areas of research to improve our understanding on terrestrial and aquatic biogeochemical  
105 cycling in northern permafrost regions. Our database contains ancillary data describing the  
106 geographical and ecological conditions associated with each DOC concentration, allowing us to  
107 reveal patterns in DOC concentrations and lability measures for 562 sampling sites across  
108 multiple ecosystem types and under varying disturbance regimes. This study represents the first  
109 systematic review of DOC concentrations within terrestrial permafrost ecosystems found in the



110 circumpolar north. As such, it provides unique and valuable insights into identifying ecoregions,  
111 or landscape characteristics, associated with the highest DOC concentrations, and thus regions  
112 with the greatest potential for DOC mobilization. Mobilization rates represent DOC loss and  
113 include specific discharge of DOC ( $\text{g DOC m}^{-2}$ ), export rate of DOC per day ( $\text{g C m}^{-2} \text{ day}^{-1}$ ) and  
114 per year ( $\text{g C m}^{-2} \text{ year}^{-1}$ ), and biodegradable DOC (BDOC; %). We hypothesized that (i) the  
115 highest DOC concentrations would be found in organic rich wetland ecosystems, (ii) disturbance  
116 would lead to increased export and biodegradability of DOC, and (iii) the most biodegradable  
117 DOC would be found in Yedoma and tundra ecosystems.

## 118 2. Methods

119 This systematic review used a methodological framework proposed by Arksey &  
120 O'Malley (2005) and follows five steps: 1) develop research questions and a search query; 2)  
121 identify relevant studies; 3) study selection; 4) data extraction; and 5) data analysis, summary,  
122 and reporting. The literature search was guided by four research questions: 1) what are the  
123 concentrations of DOC found in terrestrial ecosystems across the northern circumpolar  
124 permafrost region?; 2) what are the rates of export and/or degradation (mobilization) of DOC  
125 within these ecosystems?; 3) What are the major controls on DOC concentrations and rates of  
126 mobilization?; and 4) how are concentrations and mobilization rates impacted by thermokarst  
127 formation?

### 128 2.1 Literature Search

129 Based on *a priori* tests, we used the following search query string to find papers using  
130 information found in their title, abstract, and keywords: ("dissolved organic carbon") AND  
131 (permafrost OR thermokarst OR "thaw slump") AND (soil OR peat) AND (export OR degrad\*  
132 OR decomposition OR mineralization). We used Web of Science, Science Direct, Scopus,  
133 PubMed, and Google Scholar to generate a database of tier 1, peer-reviewed articles published  
134 between 2000 – 2022. The search function on Science Direct does not support the use of  
135 wildcards such as "\*", so "degrad\*" was changed to "degradation". We removed duplicate  
136 references found across multiple databases using Mendeley© referencing software (v1.17.1,  
137 Mendeley Ltd. 2016). Once this initial database was compiled, we used the same search query  
138 string as above to search for additional articles on the first 15 pages of Google Scholar. This



139 resulted in the addition of a further 150 articles to be included in our systematic screening  
140 process.

#### 141 *2.2 Systematic Screening of Peer-Reviewed Publications*

142 The selection of relevant studies was comprised of inclusion criteria and relevance  
143 screening in three steps. In the first step we placed limits on initial study searches in the  
144 electronic databases mentioned above. Studies were included in the review if they were primary  
145 research, published in English, and published between 2000 – 2022 (Table 1). Only quantitative  
146 studies conducted in terrestrial ecosystems within the northern circumpolar permafrost region, as  
147 defined by Brown et al., (1997), and reporting DOC concentration and mobilization rates were  
148 included. Studies not meeting these criteria were eliminated and the remaining studies proceeded  
149 to the second screening step.

Table 1. Summary of criteria used to identify suitable studies in the preliminary screening stage

	<b>Inclusion criteria</b>	<b>Exclusion criteria</b>
<b>Timeline</b>	Study published between 2000 – 2022	Study published prior to 2000
<b>Study type</b>	Primary research article published in peer-reviewed journal using quantitative methods	Thesis/dissertations and secondary research studies (reviews, commentaries, editorials)
<b>Language</b>	Published in English	Studies published in other languages
<b>Region</b>	Conducted within the northern circumpolar permafrost region	Conducted outside of the northern circumpolar permafrost region
<b>Outcome</b>	Studies on DOC concentration, export or degradation in permafrost environments	Studies not on DOC concentration, export or degradation in permafrost environments

150

151 In the second step, the primary relevance of articles was screened, based on article titles,  
152 abstracts, and keywords, and the eligibility criteria provided in Table 2. Studies deemed  
153 irrelevant were eliminated and the remaining studies proceeded to the third and final screening



154 step, or secondary screening stage, which was based on was based on more specific eligibility  
 155 criteria (Table 2) applied to the full text.

Table 2. Primary and secondary relevance screening tools. Primary screening tool used in the article title, abstract, and keyword screening stage. Secondary screening tool used in full-text screening stage

Screening stage	Screening questions	Response details
<b>Primary</b>	Does the study involve quantitative data collected from a permafrost environment?	Yes – reports on quantitative data collected from a permafrost environment  No – does not report on the above
<b>Primary and Secondary</b>	Is the study region within the northern circumpolar permafrost region?	Yes – reports on quantitative data (including field observations and lab data) collected from the circumpolar permafrost environment.  No – study region is not in the northern circumpolar permafrost regions; other examples could be mountainous permafrost or Tibetan plateau
<b>Primary and Secondary</b>	Is the article in English and NOT a review, book chapter, commentary, correspondence, letter, editorial, case report, or reflection?	Yes – study is in English and is a primary research article that includes quantitative studies (field and lab based), including model-based research as it relies on observational data.*  No – study is not in English and/or is a review, book, editorial, working paper, commentary, conference proceeding, supplementary text, or qualitative study which does not address outcomes relevant to this review
<b>Primary and Secondary</b>	Does the study involve the concentration, export or degradation of terrestrially derived DOC?	Yes – reports on terrestrial DOC concentration, export, or degradation, including concentrations and characterization  No – does not report on terrestrial DOC concentration, export, or degradation
<b>Secondary</b>	Is the article in English, longer than 500 words, and published between 2000 - 2022?	Yes – study is published between 2000 – 2022  No – study is published prior to 2000

156 \*For model-based studies, the original field/lab data used to parametrise or develop the model  
 157 was used. If this data was taken from previously published work, then those studies were used  
 158 and the model-based study removed.



159            *2.3 Database compilation*

160            A database with reported DOC concentrations and mobilization rates i.e., rates of either  
161            DOC export or degradation, was compiled using data from all studies that were deemed relevant  
162            following the study selection phase. The database was compiled to compare DOC concentrations  
163            and mobilization rates between different sites. We define a site as an area where either soil,  
164            water, or ice samples were taken from that has similar vegetation composition, water table  
165            position, permafrost regime, and was either disturbed or pristine. Site descriptions were derived  
166            from the text of each study. Where possible, individual daily measurements of DOC  
167            concentrations and mobilization rates were taken. When replicates of the same daily  
168            measurement were provided, we used the mean of those replicates, which was relevant for 10  
169            studies within the database, representing 72 DOC concentrations. All data was extracted from  
170            data tables, text, supplementary material, or extracted from data figures using WebPlotDigitizer  
171            (<https://automeris.io/WebPlotDigitizer>).

172            All studies reported measuring DOC concentrations collected from either open-water, pore  
173            water, ice, or soil using a median filter pore size of 0.45  $\mu\text{m}$  with first and third quartiles pore  
174            size of 0.45 and 0.7  $\mu\text{m}$ . Measurements from all 12 months of the year were included in the  
175            database with the majority occurring during the growing season (May – August), a small portion  
176            during the non-growing season, and the remaining sampling times were either not reported or are  
177            averages over multiple sampling occasions. We included data from studies that were both field  
178            and lab based. However, any data where a treatment was applied was excluded, except for  
179            temperature treatments during incubation experiments when assessing the biodegradability of  
180            DOC. When lab-based studies included an incubation, only Day 0 DOC concentrations were  
181            used when comparing DOC concentrations across studies. We chose to remove any DOC  
182            concentrations from samples taken below 3 m depth, which represented 3% of all DOC  
183            measurements. These measurements were removed for better comparability with the current best  
184            estimation of soil organic carbon stocks within the northern circumpolar permafrost zone  
185            (Hugelius et al., 2014). We also removed any DOC concentrations greater than 500  $\text{mg L}^{-1}$ ,  
186            which represented 2% of all DOC concentrations. Samples that were above 500  $\text{mg L}^{-1}$  and were  
187            sampled below 3 m represented 1% of all DOC concentrations.



188 Site averaged daily DOC concentrations ( $\text{mg L}^{-1}$ ) and mobilization rates were estimated from  
189 the average concentration and mobilization rates measured within a single day or sampling  
190 occasion. Repeated measurements at a site, either over the growing season or multiyear  
191 measurements, were treated as an individual estimate of DOC concentrations and mobilization  
192 rates. Other continuous variables that were similarly estimated include soil moisture, water table  
193 position, organic layer depth, active layer depth, bulk density of soil, soil carbon content (%),  
194 soil nitrogen content (%), carbon:nitrogen, pH, electrical conductivity ( $\mu\text{S cm}^{-1}$ ), specific UV  
195 absorbance at 254 nm (SUVA;  $\text{L mg C}^{-1} \text{m}^{-1}$ ), total dissolved nitrogen ( $\text{mg L}^{-1}$ ), nitrate ( $\text{mg L}^{-1}$ ),  
196 ammonium ( $\text{mg L}^{-1}$ ), chloride ( $\text{mg L}^{-1}$ ), calcium ( $\text{mg L}^{-1}$ ), and magnesium ( $\text{mg L}^{-1}$ ). Mean annual  
197 temperatures and precipitation, sampling depth, filter size, the number of days over which  
198 sampling took place, how many years following disturbance measurements were taken were also  
199 recorded. Several continuous variables other than those mentioned above were also recorded in  
200 the database, but not used for analysis if they represented  $< 20\%$  of the database. We chose 20%  
201 as the cut-off point for use in comparison of the relationship between DOC concentrations and  
202 mobilization with other site continuous variables.

203 Categorical variables included in the database were site location within the permafrost zone  
204 (continuous, discontinuous, sporadic; Brown et al., 1997) and ecoregion (arctic tundra, sub-arctic  
205 tundra, sub-arctic boreal, and continental boreal; (Olson et al., 2001). We included site surface  
206 permafrost conditions (present or absent), the thermal horizon layer sampled (active layer,  
207 permafrost, permafrost free, water, and thaw stream), and if present what type of disturbance  
208 occurred at the site (fire, active layer thickening, thermokarst terrestrial, or thermokarst aquatic).  
209 We also included the soil class found at the site (Histel, Histosol, Orthel, and Turbel; USDA,  
210 1999) and whether the DOC was from the organic or mineral soil. To assess the influence of  
211 sampling approach and method of analysis, we included method of DOC extraction  
212 (centrifugation of soil sample, leaching of soil, dialysis, grab sample, ice core extraction,  
213 potassium sulphate extraction, lysimeter, piezometer, pump, rhizons) and DOC measurement  
214 method (combustion, persulphate, photometric, or solid-phase extraction).

215 Sites were classified according to ecosystem type, and these included coastal tundra, forest,  
216 peatland, permafrost bog, permafrost wetland, retrogressive thaw slump, upland tundra, and  
217 Yedoma. Ecosystem classification is based on the general site description in the article, the



218 provided ecosystem classification within the article, and site data including vegetation  
219 composition, permafrost conditions, and ecoregion. Yedoma sites include pristine forest, upland  
220 tundra, and coastal tundra, as well as retrogressive thaw slumps and other thermokarst features  
221 found within the Yedoma permafrost domain (Strauss et al., 2021). The ecosystem classification  
222 retrogressive thaw slump only includes these thermokarst features found outside the Yedoma  
223 permafrost domain. Each ecosystem type was further classified based on the type of permafrost  
224 thaw or thermokarst formation that occurred there. These thaw or thermokarst types included  
225 thermokarst bog, thermokarst wetland, active layer thickening, retrogressive thaw slump,  
226 exposure, thermo-erosion gully, and active layer detachment.

#### 227 *2.4 Database analysis*

228 All statistical analyses were carried out in R (Version 3.4.4, R Core Team, 2015). We used  
229 Kruskal-Wallis analysis to test for differences in median DOC concentrations among various  
230 categorical variables such as permafrost zones, ecoregions, soil class, thermal horizon, and  
231 ecosystems. Post-hoc comparisons of median DOC concentrations among these categories were  
232 performed using pairwise Wilcox test. We used ANOVAs and Bonferroni post-hoc tests on  
233 linear mixed effects models, that include ecosystem type as a random factor, to evaluate  
234 significant differences in DOC concentrations between methods of DOC extraction and  
235 measurement. For regression analysis, data was transformed using a Box Cox transformation and  
236 the optimal  $\lambda$  using the *MASS* package (Ripley et al., 2019). We used analysis of covariance  
237 (ANCOVA) to test for differences in DOC concentrations in different thermal horizons (i.e.,  
238 active layer and intact permafrost lens) between ecosystem types, while controlling for the month  
239 in which sampling occurred. Permafrost lens DOC concentrations are determined from soil and  
240 pore water within the permafrost layer and extracted via frozen cores, whereas active layer  
241 samples are taken from soil cores or porewater that are unfrozen at the time of sampling. We  
242 used partial least squares regression (PLS) to assess the performance of continuous and  
243 categorical variables in predicting DOC concentrations. Predictor variables were categorized  
244 based on their Variable Importance in Projections (VIP) method in the *plsVarSel* package  
245 (Mehmood et al., 2012), whereby variables with a score  $> 1$  are deemed to be significant. PLS  
246 was performed using the *pls* package (Mevik & Wehrens, 2007) and we chose to use PLS as it is  
247 tolerant of co-correlation of predictor variable, deviations from normality, and missing values, all



248 of which were found within the database. In the PLS ecosystem classes were subdivided into  
249 pristine or disturbed (i.e., impacted by permafrost thaw). Pristine sites were further subdivided  
250 by the thermal horizon in which the DOC concentrations were measured (active layer and  
251 permafrost lens). To evaluate the change in ecosystem DOC concentrations following  
252 thermokarst formation, based on all studies from the systematic review, we calculated the  
253 response ratio using the *SingleCaseES* package (Pustejovsky et al., 2021). We define thermokarst  
254 as the process by which ice-rich permafrost deposits undergo complete thaw, resulting in surface  
255 subsidence and the formation of a new, thermokarst feature that is ecological different regarding  
256 water table position, redox conditions, and vegetation type, from the preceding pristine  
257 ecosystem. Very few studies in our database report DOC concentrations for both pristine and  
258 thermokarst affected ecosystem (< 20 %). To include as much data as possible we chose an  
259 effect size metric that is unlikely to be influenced by studies with large sample number and  
260 variance. The response ratio is;

261 
$$\text{Pristine to Thermokarst Effect Response ratio} = \ln\left(\frac{X_P}{X_T}\right) \quad \text{Eqn. 1}$$

262 where  $X_P$  = mean DOC concentration of pristine ecosystems and  $X_T$  = mean DOC concentration of  
263 thermokarst effected ecosystems (Lajeunesse, 2011). This represents the log proportional  
264 difference in mean DOC concentrations between thermokarst and pristine ecosystems, where a  
265 positive response ratio indicates a decrease in DOC concentrations following thermokarst. The  
266 distribution of the data was inspected visually and with the Shapiro–Wilk test. We tested  
267 homogeneity of variances using the *car* package and Levene’s test (Fox and Weisberg, 2011).  
268 We report uncertainty using the interquartile range (lower, median, and upper quartiles), except  
269 for response ratios which we report as  $\pm$  95% confidence intervals. We here define the statistical  
270 significance level at 5%.

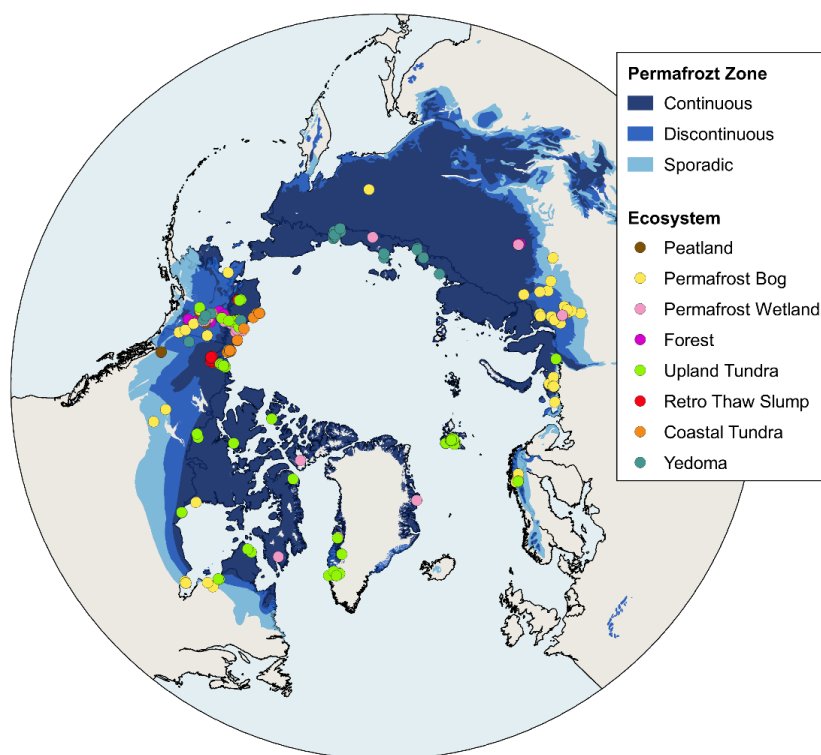
### 271 **3. Results**

#### 272 *3.1 Database generation*

273 Our initial search using Web of Knowledge, Science Direct, Scopus, PubMed, and  
274 Google Scholar returned a total of 577 unique papers published between 2000 – 2022 that assess  
275 the concentrations and rates of mobilization of DOC in terrestrial ecosystems within the northern



276 circumpolar permafrost region. Of these initial 577 studies, 111 remained after the systematic  
277 screening process (Table 1 & 2). From these 111 studies we generated our database. The final  
278 database of 111 studies contained a total of 3,340 DOC concentrations ( $\text{mg L}^{-1}$ ), with 2,845 DOC  
279 concentrations between 0 – 500  $\text{mg L}^{-1}$ , found within the top 3 m of permafrost soils from field  
280 and lab-based studies (using only Day 0 lab-based DOC concentrations). These concentrations  
281 were taken from 562 different sampling locations, representing 8 different ecosystem types  
282 (Figure 1) across the northern circumpolar permafrost region. All studies except, for one  
283 (Olefeldt et al., 2012), reported DOC concentrations.



284

285 Figure 1. Map of sampling locations where DOC measurements ( $n=562$ ) from the top 3 m for  
286 each ecosystem type. In many cases, the same sampling location was used in multiple studies  
287 leading to some overlap, therefore the number of sampling sites included in the data set (562)  
288 are not all clearly identifiable from this map. Retro Thaw Slump = Retrogressive Thaw Slump.  
289 Blue shading represents permafrost zonation (Brown et al., 1997).

290



291 The final database contained a considerably lower number of DOC mobilization  
292 measurements. The database includes 16 measurements of specific discharge of DOC (g DOC m<sup>-2</sup>  
293 <sup>2</sup>) from 3 studies, 9 export rate of DOC per day (g C m<sup>-2</sup> day<sup>-1</sup>) and per year (g C m<sup>-2</sup> year<sup>-1</sup>)  
294 measurements were each found in 2 studies. The number of specific discharge, export of DOC  
295 per day, and export of DOC per year measurements combined were <1% of the number of DOC  
296 concentration measurements. As such they were not considered for analysis of DOC  
297 mobilization. A total of 146 BDOC (%) measurements, 4% of the total number of DOC  
298 concentration measurements, were found in 14 studies. These measurements of BDOC were  
299 from Yedoma (30:5, number of measurements:studies), Upland Tundra (55:5), Forest (18:3),  
300 Permafrost Wetland (12:2), and Permafrost Bog (31:5) ecosystems. Given the low number of  
301 other forms of DOC mobilization and relatively comparable spread of BDOC measurements  
302 across ecosystem types, we chose to include BDOC measurements in our analysis despite a low  
303 total number of measurements compared to DOC concentrations, and we consider this lower  
304 sample size during our interpretation of results.

305 Filter size used in studies ranged from 0.15 – 0.7 µm. The majority of studies used a filter  
306 size of 0.45 µm (1,375 out of 2,845 DOC measurements), 0.7 µm was the second most common  
307 filter size (n = 489), followed by 0.22 µm (n = 332) and 0.6 µm (n = 143). Two studies used a  
308 filter size of 0.15 µm totalling 18 DOC measurements and remaining studies (n = 12) did not  
309 provide a filter size. DOC concentrations were found to differ between different filter sizes  
310 (ANOVA:  $F_{(4, 2339)} = 22.9, p < 0.001$ ). DOC concentrations from samples filtered using 0.7 µm  
311 were lower (median = 11 mg L<sup>-1</sup>) than 0.45 µm and 0.22 µm filtered samples (median = 53 and  
312 42 mg L<sup>-1</sup>, respectively). We consider the effects of filter size to be minor. DOC concentrations  
313 were found to be significantly different between samples subject to the 11 different extraction  
314 methods used (ANOVA:  $F_{(10, 2515)} = 21.8, p < 0.001$ ), and between water based and soil (solid)  
315 based extraction methods (ANOVA:  $F_{(1, 2524)} = 182.1, p < 0.001$ ). Median DOC concentrations of  
316 the 4 methods of extraction directly from soils (leaching from soil under field moisture  
317 conditions, leached from dried soils, centrifuged soils, and extracted using K<sub>2</sub>SO<sub>4</sub>) were 57 mg  
318 L<sup>-1</sup>, with upper and lower quartiles of 20 and 120 mg L<sup>-1</sup>, respectively. The 7 water-based  
319 extraction methods had a median DOC concentration of 24 mg L<sup>-1</sup>, with upper and lower  
320 quartiles of 8 and 59 mg L<sup>-1</sup>, respectively. DOC concentrations differed (ANOVA:  $F_{(3, 2515)} =$



321 36.2,  $p < 0.001$ ) between samples subject to different dissolved organic carbon measurement  
322 methods, with median values of 37 and 48 mg L<sup>-1</sup> for the combustion, and photometric methods,  
323 respectively. Median values measured using the persulphate were higher at 97 mg L<sup>-1</sup>.  
324 Combustion was the most common method, accounting for 2,170 DOC concentrations, followed  
325 by persulphate ( $n = 230$ ) and photometric ( $n = 31$ ). In this study we did not focus on  
326 systematically testing the effect of filter sizes, extraction methods, or DOC measurement  
327 methods. Our goal was to assess the concentration and mobilization of DOC in terrestrial  
328 permafrost ecosystems and the assessment of methods is outside the scope of our study. Rather,  
329 we compare DOC concentrations collected from samples using a variety of these methods and  
330 suggest that future studies use this information to decide on methods to be consistent with  
331 compiled measurements, thus far.

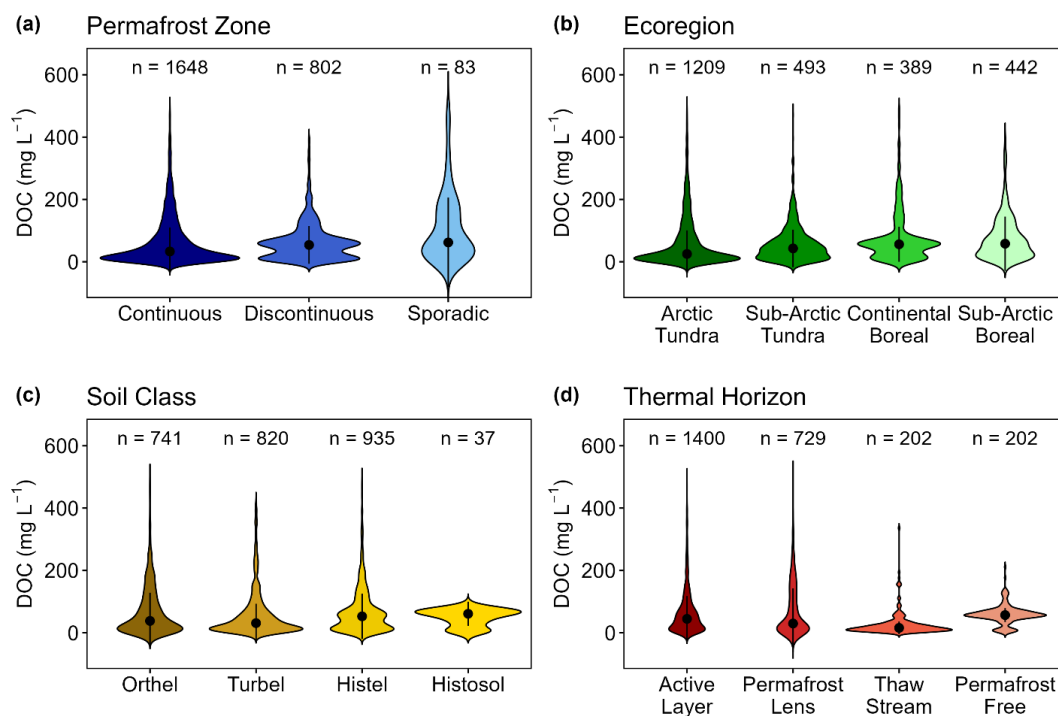
### 332 3.2 DOC concentrations and study regions

333 Upon inspection of DOC concentrations in the database, we determined that the data was  
334 non-normally distributed. The DOC concentrations were skewed toward the lower end of our 0 –  
335 500 mg L<sup>-1</sup> range; thus, we report median, upper, and lower quartiles below. Across all studies,  
336 within the top 3 m, the median DOC concentration was 41 mg L<sup>-1</sup>, with upper and lower  
337 quartiles of 12 and 86 mg L<sup>-1</sup>, respectively. DOC concentrations were found to differ among the  
338 three permafrost zones (chi-square = 32,  $df = 2$ ,  $p < 0.001$ ; Figure 2a). The highest median DOC  
339 concentrations were found within the sporadic permafrost zone ( $n = 83$ ; 62 mg L<sup>-1</sup>), lower  
340 quartile (LQ) and upper quartile (UQ) of 23 and 167 mg L<sup>-1</sup>, respectively. The lowest median of  
341 33 mg L<sup>-1</sup> (LQ and UQ of 11 and 88 mg L<sup>-1</sup>, respectively) was found in the continuous  
342 permafrost zone ( $n = 1,648$ ), with the greatest density of samples having lower DOC  
343 concentrations than observed in the violin plots of both the discontinuous and sporadic (Figure  
344 2a). This change in DOC concentration's along the latitudinal gradient of the permafrost zonation  
345 was also seen in the latitudinal gradient associated with ecoregion (chi-square = 78,  $df = 3$ ,  $p <$   
346  $0.001$ ; Figure 2b). The highest DOC concentrations were found in the continental boreal ( $n =$   
347  $389$ ; 56 mg L<sup>-1</sup>; LQ = 24 mg L<sup>-1</sup>; UQ = 80 mg L<sup>-1</sup>) and Sub-Arctic Boreal ( $n = 442$ ; 58 mg L<sup>-1</sup>;  
348 LQ = 20 mg L<sup>-1</sup>; UQ = 107 mg L<sup>-1</sup>) ecoregions, and lowest in the Arctic Tundra ( $n = 1,209$ ; 25  
349 mg L<sup>-1</sup>; LQ = 9 mg L<sup>-1</sup>; UQ = 84 mg L<sup>-1</sup>) and Sub-Arctic Tundra ( $n = 493$ ; 43 mg L<sup>-1</sup>; LQ = 15  
350 mg L<sup>-1</sup>; UQ = 76 mg L<sup>-1</sup>) ecoregions. Inspection of the distribution of DOC concentrations across



351 the ecoregions highlights that the Arctic Tundra ecoregion had the highest density of samples at  
352 the lowest DOC concentration (Figure 2b).

353 These latitudinal differences are also reflected in the observed differences (chi-square =  
354 20,  $df = 3$ ,  $p < 0.001$ ) in DOC concentrations found within different soil classes. The highest  
355 DOC concentrations are found within organic rich Histosol ( $n = 37$ ;  $61 \text{ mg L}^{-1}$ ;  $LQ = 32 \text{ mg L}^{-1}$ ;  
356  $UQ = 71 \text{ mg L}^{-1}$ ) and Histel soils ( $n = 935$ ;  $53 \text{ mg L}^{-1}$ ;  $LQ = 16 \text{ mg L}^{-1}$ ;  $UQ = 88 \text{ mg L}^{-1}$ ; Figure  
357 2c), with the distribution of the data from these soils types having a higher density at greater  
358 DOC concentrations (Figure 2c). Histel and Histosol soils are the main type of permafrost soil  
359 found within the sporadic and discontinuous permafrost zone and both boreal ecoregions  
360 (Hugelius et al., 2014). Mineral rich Orthels ( $n = 741$ ;  $38 \text{ mg L}^{-1}$ ;  $LQ = 11 \text{ mg L}^{-1}$ ;  $UQ = 102 \text{ mg}$   
361  $\text{L}^{-1}$ ) and Turbels ( $n = 820$ ;  $31 \text{ mg L}^{-1}$ ;  $LQ = 12 \text{ mg L}^{-1}$ ;  $UQ = 74 \text{ mg L}^{-1}$ ), mineral permafrost  
362 soils that have experienced cryoturbation, had the lowest DOC concentrations. The median DOC  
363 concentrations found within the top 3 m of these soil classes represent  $<1\%$  of the soil organic  
364 carbon stock found in the top 3 m of each soil class (Hugelius et al., 2014). DOC concentrations  
365 also differed within the thermal horizon of these different soil classes (chi-square = 91,  $df = 3$ ,  $p$   
366  $< 0.001$ ; Figure 2d). The highest DOC concentrations were found in permafrost free sites ( $n =$   
367  $202$ ;  $57 \text{ mg L}^{-1}$ ;  $LQ = 47 \text{ mg L}^{-1}$ ;  $UQ = 69 \text{ mg L}^{-1}$ ), which were largely Histosol soils (19%) or  
368 Histel soils (74%) that have experienced thermokarst formation. In areas where permafrost was  
369 present, DOC concentrations were highest in the active layer ( $n = 1,400$ ;  $45 \text{ mg L}^{-1}$ ;  $LQ = 14 \text{ mg}$   
370  $\text{L}^{-1}$ ;  $UQ = 88 \text{ mg L}^{-1}$ ) and the permafrost lens ( $n = 729$ ;  $30 \text{ mg L}^{-1}$ ;  $LQ = 10 \text{ mg L}^{-1}$ ;  $UQ = 123$   
371  $\text{mg L}^{-1}$ ).



372

373 Figure 2. Violin plots of DOC concentrations ( $\text{mg L}^{-1}$ ) found in the top 3 m across (a) permafrost  
374 zones, (b) ecoregions, (c) soil classes, and (d) thermal horizons. (a) Dark to light blue shading  
375 represents the permafrost zones Continuous, Discontinuous, and Sporadic, according to Brown  
376 et al., (1997). (b) Dark to light green shading represents the ecoregions Arctic Tundra, Sub-  
377 Arctic Tundra, Continental Boreal, and Sub-Arctic Boreal, according to Olson et al., (2001). (c)  
378 Dark to light yellow shading represents the soil classes Histosol, Histel, Orthel, and Turbel,  
379 according to the USDA Soil Taxonomy (USDA, 1999). Histosols are organic rich, non-  
380 permafrost soil. Histels, Orthels, and Turbels are permafrost-affected soils (Gelisol order).  
381 Histels are organic rich, Orthels are non cryoturbated affected mineral soils, and Turbels are  
382 cryoturbated permafrost soils. (d) Dark to light red shading represents the thermal horizons  
383 Active Layer, Permafrost Lens, Thaw Stream, and Permafrost Free. Active layer represents the  
384 seasonally unfrozen soil layer above the permafrost layer. Permafrost Lens represents the  
385 permanently frozen (below  $0^{\circ}\text{C}$ ) layer. Thaw Stream represents flowing surface waters following  
386 permafrost thaw. Permafrost Free represents areas that are not underlain by permafrost. Black  
387 dots on each violin plot represents the median. Black vertical lines represent the interquartile  
388 range with the upper and lower limits representing the 75<sup>th</sup> and 25<sup>th</sup> percentiles, respectively.  
389 Either side of the black vertical line represents a kernel density estimation. This shape shows  
390 the distribution of the data, with wider areas representing a higher probability that samples  
391 within the database will have that DOC concentrations. The number of samples (n) found in  
392 each sub-category is found above each corresponding violin plot.

393

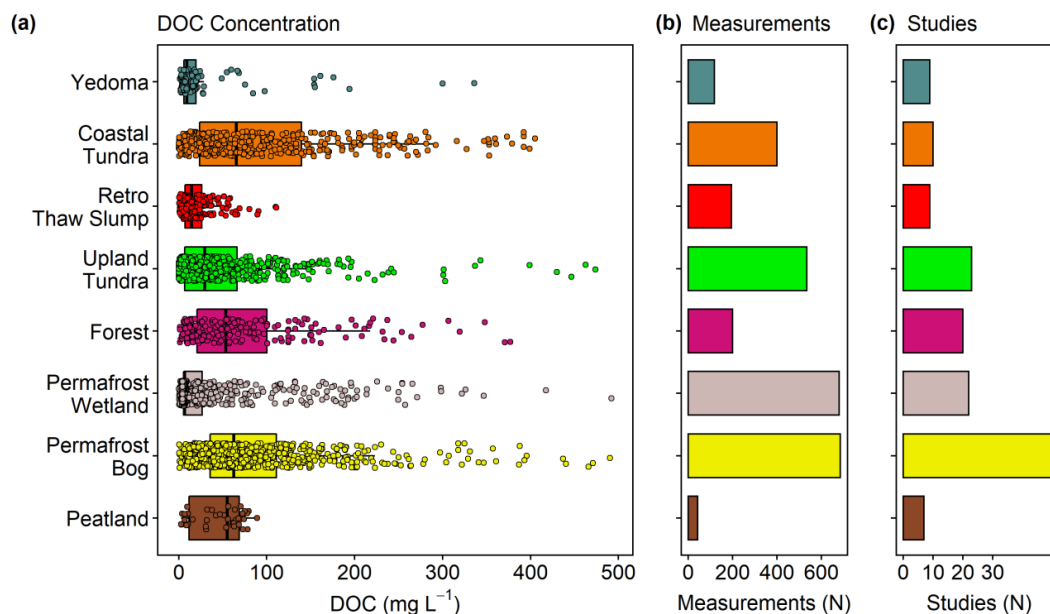


394            *3.3 Trends in DOC concentrations across ecosystems*

395            Similar to other categorical variables (i.e. permafrost zone, ecoregion, soil class, and  
396 thermal horizon data), DOC concentrations within each of the eight ecosystem types were found  
397 to be non-normally distributed, with median values skewed toward the lower end of the 0 – 500  
398 mg L<sup>-1</sup> range of concentrations (Figure A1). Permafrost bogs and permafrost wetlands were the  
399 most represented in the database with regards to DOC concentrations, with a total of 685  
400 concentrations from 38 studies and 679 concentrations from 22 studies, respectively. The  
401 majority of permafrost bog measurements came from studies with field sites within Canada  
402 (Figure 1), as was the case for upland tundra and retrogressive thaw slump DOC concentration  
403 data. The majority of permafrost wetland sample locations were found in Russia, whereas the  
404 majority of the 399 coastal tundra sampling locations were in the USA. The least represented  
405 ecosystem classes included the peatland ecosystem class, which is not strictly a permafrost  
406 ecosystem as the other are, and the Yedoma ecosystem class (118 DOC concentrations from 9  
407 studies). DOC concentrations differed significantly across the eight ecosystem types (chi-square  
408 = 700, df = 7,  $p < 0.001$ ; Figure 3). The highest DOC concentrations were found in coastal  
409 tundra (66 mg L<sup>-1</sup>; LQ = 24 mg L<sup>-1</sup>; UQ = 140 mg L<sup>-1</sup>) and permafrost bogs (63 mg L<sup>-1</sup>; LQ = 36  
410 mg L<sup>-1</sup>; UQ = 111 mg L<sup>-1</sup>) ecosystems. The lowest DOC concentrations were found in  
411 permafrost wetlands (7 mg L<sup>-1</sup>; LQ = 6 mg L<sup>-1</sup>; UQ = 26 mg L<sup>-1</sup>) and Yedoma ecosystems (9 mg  
412 L<sup>-1</sup>; LQ = 2 mg L<sup>-1</sup>; UQ = 20 mg L<sup>-1</sup>), both of which had only slightly lower median DOC  
413 concentrations than retrogressive thaw slumps (15 mg L<sup>-1</sup>; LQ = 7 mg L<sup>-1</sup>; UQ = 26 mg L<sup>-1</sup>).



414



415

416 Figure 3. Boxplot and jitter plot of (a) DOC concentrations (mg L<sup>-1</sup>), (b) the number of DOC  
417 measurements, and (c) number of studies including DOC measurements were taken from the  
418 top 3 m for each ecosystem type. Retro Thaw Slump = Retrogressive Thaw Slump. Boxes  
419 represents the interquartile range (25 – 75%), with median shown as black horizontal line.  
420 Whiskers extend to 1.5 times the interquartile range (distance between first and third quartile)  
421 in each direction. Jitter points represent the concentration of each individual DOC measurement,  
422 with random variation applied to each points location vertically in the plot, to avoid overplotting.  
423 Yedoma = dark teal. Coastal Tundra = orange. Retro Thaw Slump = red. Upland Tundra =  
424 green. Forest = purple. Permafrost Wetland = light pink. Permafrost bog = yellow. Peatland =  
425 brown.

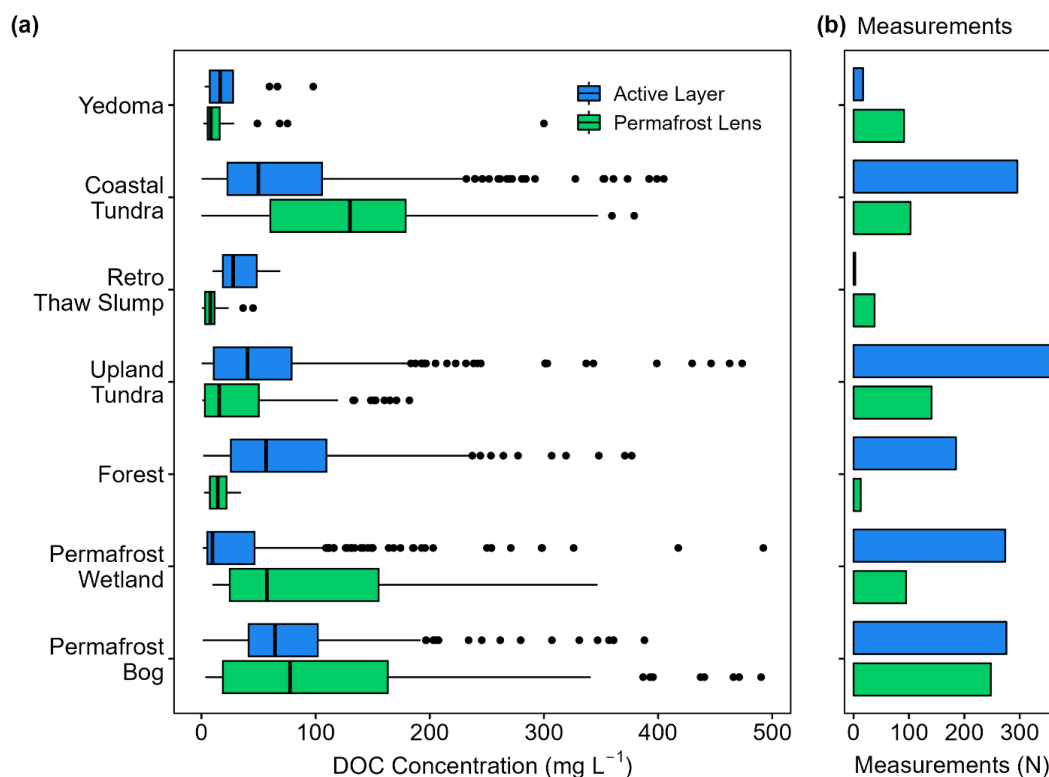
426

427 When grouping all DOC concentrations by ecosystem types and differentiating between  
428 the active layer and permafrost lens thermal horizons, we found that DOC concentrations  
429 differed between the active layer and permafrost for all ecosystems (ANCOVA:  $F_{(1, 1277)} = 49.8$ ,  
430  $p < 0.001$ ) except for permafrost bogs (chi-square = 0.37,  $df = 1$ ,  $p = 0.5$ ) and Yedoma (chi-  
431 square = 3.5,  $df = 1$ ,  $p = 0.06$ ) ecosystems (Figure 4). Within the permafrost lens thermal  
432 horizon, the highest DOC concentrations were found in coastal tundra ( $n = 103$ ;  $130 \text{ mg L}^{-1}$ ; LQ  
433 =  $60 \text{ mg L}^{-1}$ ; UQ =  $179 \text{ mg L}^{-1}$ ) and permafrost bogs ( $n = 248$ ;  $78 \text{ mg L}^{-1}$ ; LQ =  $19 \text{ mg L}^{-1}$ ; UQ =  
434  $163 \text{ mg L}^{-1}$ ) sites, and lowest found in Yedoma sites ( $n = 91$ ;  $8 \text{ mg L}^{-1}$ ; LQ =  $6 \text{ mg L}^{-1}$ ; UQ =  $16$



435  $\text{mg L}^{-1}$ ). The highest active layer DOC concentrations were in permafrost bogs ( $n = 276$ ;  $64 \text{ mg}$   
436  $\text{L}^{-1}$ ;  $\text{LQ} = 41 \text{ mg L}^{-1}$ ;  $\text{UQ} = 102 \text{ mg L}^{-1}$ ) and forest ( $n = 185$ ;  $57 \text{ mg L}^{-1}$ ;  $\text{LQ} = 26 \text{ mg L}^{-1}$ ;  $\text{UQ} =$   
437  $110 \text{ mg L}^{-1}$ ) sites, and lowest found in permafrost wetland sites ( $n = 274$ ;  $10 \text{ mg L}^{-1}$ ;  $\text{LQ} = 5 \text{ mg}$   
438  $\text{L}^{-1}$ ;  $\text{UQ} = 47 \text{ mg L}^{-1}$ ).

439



440

441 Figure 4 . Boxplot of (a) DOC concentrations ( $\text{mg L}^{-1}$ ) and (b) (b) the number of DOC  
442 measurements in the Active Layer and Permafrost Lens thermal horizons of each ecosystem  
443 type. Only DOC concentrations from ecosystems with these thermal horizons present is used,  
444 thus no peatland or permafrost-free sites are included. Retro Thaw Slump = Retrogressive  
445 Thaw Slump. Boxes represents the interquartile range (25 – 75%), with median shown as black  
446 horizontal line. Whiskers extend to 1.5 times the interquartile range (distance between first and  
447 third quartile) in each direction. Blue boxplots represent DOC concentrations in the active layer.  
448 Gren boxplots represent DOC concentrations in the permafrost lens.

449

### 450 3.4 Drivers of DOC concentrations



451 No continuous variables recorded in the dataset were available for all DOC concentration  
452 database entries, with no sites containing data for all continuous variables. This limited our  
453 ability to explore relationships between continuous environmental and ecological data and DOC  
454 concentrations across the permafrost region. To address drivers of DOC concentrations across  
455 the circumpolar permafrost region we used partial least squares regression (PLS) as it is tolerant  
456 to missing values. Multiple PLS regressions were run using various combinations of continuous  
457 and categorical data with similar model performance throughout. We chose the PLS to predict  
458 DOC concentrations using environmental continuous variables and ecosystem type as this  
459 contained the lowest background correlation. The most parsimonious PLS regression extracted 5  
460 significant components, captured 79% variation of the predictor variables, and explained 37% of  
461 the variance in DOC concentrations in the dataset. The majority of the variance in DOC (35%) is  
462 explained along the first two axes of the model. The model was robust and not overfitted as  
463 model predictability was moderate ( $Q^2 = 0.35$ ) and background correlation was low (0.006).

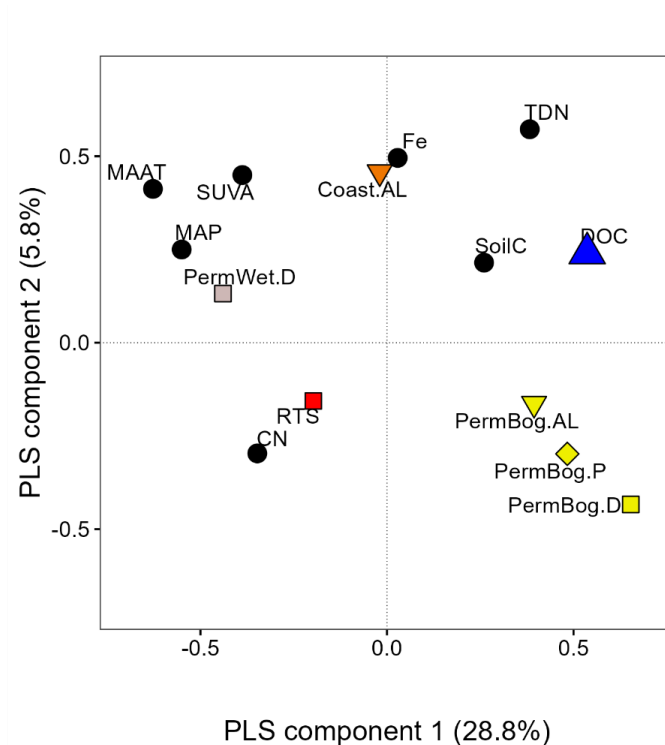
464 The PLS plot (Figure 5a) shows the correlation between DOC concentrations and  
465 selected environmental and ecological variables for the first two axes of the model. The two  
466 variables with the greatest positive and negative effect on DOC concentrations were total  
467 dissolved nitrogen content ( $\text{mg L}^{-1}$ ) and C:N ratios, respectively (Figure 5b). The positive  
468 relationship between DOC and total dissolved nitrogen soil carbon content (SoilC), and negative  
469 relationship with the specific UV absorbance at 254 nm (SUVA), may be a result of ecosystem  
470 properties. The aromatic content of organic matter is positively correlated with SUVA (Weishaar  
471 et al., 2003), with high SUVA values being used as an indication of high aromatic content  
472 (Hansen et al., 2016). Ratios of C:N have been shown to be a good proxy for decomposition  
473 (Biester et al., 2014), where high C:N values indicate higher decomposition. The strong negative  
474 relationship with C:N ratios indicates that DOC concentrations decrease with increased  
475 decomposition. Other than higher soil carbon content (SoilC) in permafrost bogs, there was no  
476 clear or obvious trends in SoilC, TDN, C:N ratios, and SUVA across ecosystem types (Figure  
477 A3). The PLS demonstrates that ecosystem type strongly affects DOC concentrations, with DOC  
478 positively related with the highest ecosystems where the highest DOC concentrations are  
479 observed, permafrost bogs and coastal tundra, and negatively related to the lower DOC  
480 ecosystems, permafrost wetland and retrogressive thaw slumps (Figure 5). This negative



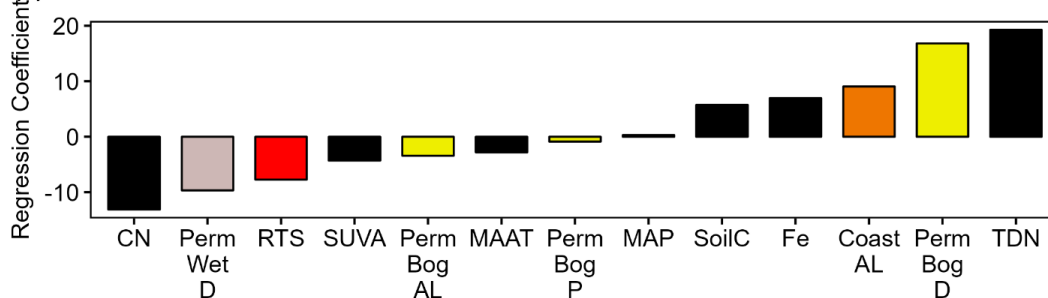
481 relationship may be due to the higher latitudes these ecosystems are generally found at, which is  
 482 supported by the negative relationship with DOC and the climate indicators mean annual  
 483 temperature (MAAT) and mean annual precipitation (MAP). Additionally, it may be due to the  
 484 high number of thermokarst affected sites found within these ecosystem classes, particularly  
 485 retrogressive thaw slumps. There is a clear negative relationship between DOC concentrations  
 486 and disturbed permafrost wetlands, retrogressive thaw slumps, and permafrost bogs.

487

(a)



(b)



488



489 Figure 5. Partial least squares regression (PLS) (a) loadings plot explaining 37% of the  
490 variability observed in DOC concentrations. PLS component axis 1 explains 28.8% of this  
491 variability, whereas PLS component axis 2 explains 5.8%. The remaining axes explain the  
492 variability in DOC are not shown for clarity. (b) Bar plot of PLS regression coefficients showing  
493 the relative importance of each variable in predicting DOC concentrations. Regression  
494 coefficients on y-axis are normalized so their absolute sum is 100, with positive and negative  
495 values indicating the direction of the relationship. In the loadings plot squares depict ecosystem  
496 classes and the blue triangle represents DOC concentrations. Black circles in the (a) loadings  
497 plot and black bars in the (b) bar plot represent continuous environmental data that had at least  
498 20% coverage of DOC data,. All continuous data was log transformed, mean centered, and  
499 standardized. Continuous data variables are represented by the colour black. CN =  
500 carbon:nitrogen ratio. SUVA = the specific UV absorbance at 254 nm ( $\text{L mg C}^{-1} \text{m}^{-1}$ ). MAP =  
501 mean annual precipitation (mm). MAAT = mean annual temperature. SoilC = carbon content of  
502 soil ( $\text{g C kg}^{-1}$ ). TDN = total dissolved nitrogen ( $\text{mg L}^{-1}$ ). Fe = dissolved iron ( $\text{mg L}^{-1}$ ). PermWet.D  
503 = disturbed permafrost wetland ecosystem class and is light pink (as in Figure 3) to represent  
504 this ecosystem class. RTS = retrogressive thaw slump ecosystem class and is red (as in Figure  
505 3) to represent this ecosystem class. Coast.AL = active layer of coastal tundra ecosystem class  
506 and is orange (as in Figure 3) to represent this ecosystem class. PermBog.AL = active layer of  
507 permafrost bog ecosystem class and is yellow (as in Figure 3) to represent this ecosystem  
508 class. PermBog.P = permafrost lens of permafrost bog ecosystem class and is yellow (as in  
509 Figure 3) to represent this ecosystem class. PermBog.D = disturbed permafrost bog ecosystem  
510 class and is yellow (as in Figure 3) to represent this ecosystem class.

### 511 3.5 Response and mobilization of DOC and BDOC to thermokarst formation

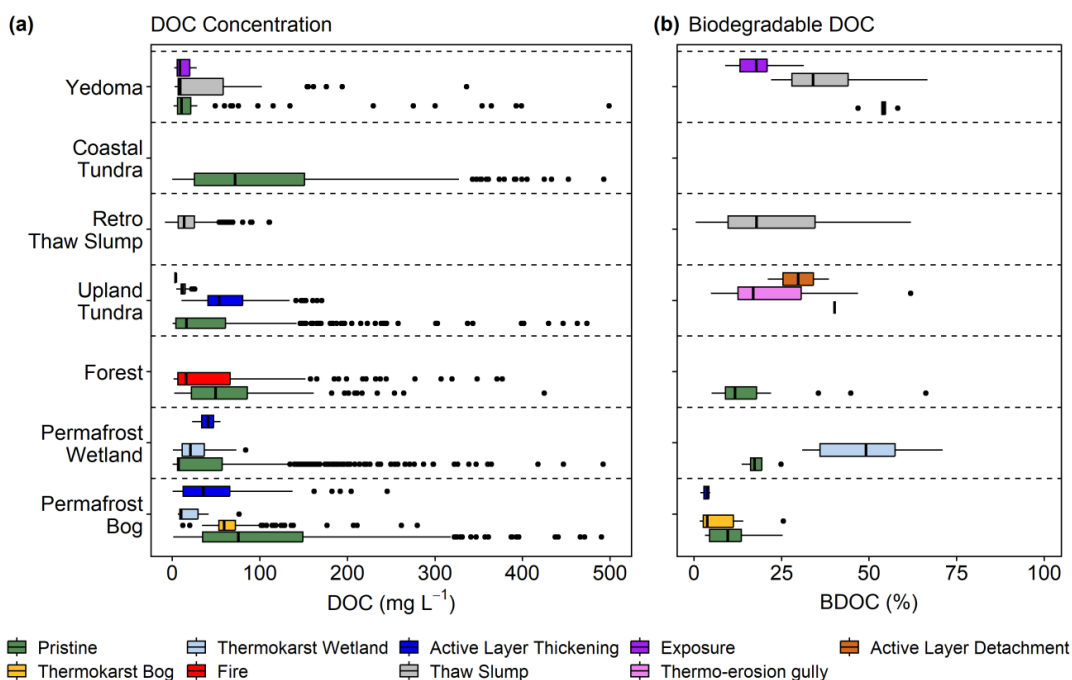
512 The highest DOC concentrations were found in pristine permafrost bog ( $75 \text{ mg L}^{-1}$ ; LQ =  
513  $37 \text{ mg L}^{-1}$ ; UQ =  $149 \text{ mg L}^{-1}$ ,  $n = 442$ ) and coastal tundra ecosystems ( $72 \text{ mg L}^{-1}$ ; LQ =  $25 \text{ mg L}^{-1}$ ;  
514  $151 \text{ mg L}^{-1}$ ; UQ =  $151 \text{ mg L}^{-1}$   $n = 427$ ; Figure 6a). No thermokarst affected coastal tundra ecosystems were  
515 recorded within the dataset. Whereas, in permafrost bogs DOC concentrations were found to  
516 differ across different thermokarst disturbances (ANOVA:  $F_{(3, 720)} = 23.04$ ,  $p < 0.001$ ), with the  
517 lowest found in thermokarst wetlands ( $10 \text{ mg L}^{-1}$ ; LQ =  $9 \text{ mg L}^{-1}$ ; UQ =  $30 \text{ mg L}^{-1}$ ,  $n = 16$ ). DOC  
518 concentrations were also found to differ between thermokarst affected and pristine sites in  
519 upland tundra ecosystems (ANOVA:  $F_{(3, 539)} = 5.91$ ,  $p < 0.001$ ). The highest DOC  
520 concentrations in upland tundra ecosystems were found in sites that had experienced active layer  
521 thickening ( $53 \text{ mg L}^{-1}$ ; LQ =  $41 \text{ mg L}^{-1}$ ; UQ =  $80 \text{ mg L}^{-1}$ ,  $n = 142$ ), whereas the lowest were  
522 found in sites that had experienced active layer detachment ( $4 \text{ mg L}^{-1}$ ; LQ =  $3 \text{ mg L}^{-1}$ ; UQ =  $5$   
523  $\text{mg L}^{-1}$ ,  $n = 6$ ). Pristine sites had the highest DOC concentrations in both Yedoma ( $11 \text{ mg L}^{-1}$ ;  
524 LQ =  $6 \text{ mg L}^{-1}$ ; UQ =  $21 \text{ mg L}^{-1}$ ,  $n = 114$ ) and forest ( $49 \text{ mg L}^{-1}$ ; LQ =  $22 \text{ mg L}^{-1}$ ; UQ =  $86 \text{ mg L}^{-1}$ ;  
525  $1$ ,  $n = 189$ ) ecosystems. However, in permafrost wetland ecosystems pristine sites had the lowest  
526 DOC concentrations ( $7 \text{ mg L}^{-1}$ ; LQ =  $6 \text{ mg L}^{-1}$ ; UQ =  $57 \text{ mg L}^{-1}$ ,  $n = 766$ ) with sites that were



527 affected by both thermokarst wetland formation ( $21 \text{ mg L}^{-1}$ ; LQ =  $11 \text{ mg L}^{-1}$ ; UQ =  $37 \text{ mg L}^{-1}$ , n  
528 = 17) and active layer thickening ( $41 \text{ mg L}^{-1}$ ; LQ =  $34 \text{ mg L}^{-1}$ ; UQ =  $47 \text{ mg L}^{-1}$ , n = 12) having  
529 higher DOC concentrations.

530 BDOC was found to differ between thermokarst disturbances within ecosystem types in  
531 only Yedoma (ANOVA:  $F_{(2, 27)} = 23.09$ ,  $p < 0.001$ ) and permafrost wetland (ANOVA:  $F_{(1, 10)} =$   
532  $15.87$ ,  $p < 0.001$ ) ecosystems. The highest BDOC was found in both of these ecosystem types  
533 also, with 54% (n = 5) in pristine Yedoma sites and 49% (n = 8) in thermokarst wetland affected  
534 permafrost wetland sites (Figure 6b), with the latter exhibiting the highest BDOC across all  
535 permafrost affected sites followed by thaw slumps (18%, n = 11) in Yedoma ecosystems and  
536 active layer thickening (40%, n = 1) in upland tundra sites. The lowest median BDOC of 4%  
537 were seen in thermokarst bogs (n = 5) and active layer thickening (n = 3) affected sites, with  
538 pristine sites experiencing BDOC of 9% (n = 15). However, not all ecosystem types in the  
539 database had BDOC data for both pristine and disturbance sites. For example, only pristine sites  
540 data was available for forests, whereas there was no pristine site data available for upland tundra  
541 sites. No BDOC data was available for coastal tundra sites.

542 All ecosystem types that had BDOC data, reported BDOC observed following 40 – 90  
543 incubation days, and this also corresponded to the highest BDOC values for each ecosystem type  
544 (Figure A4). When comparing the greatest BDOC observed within this incubation length  
545 window, we found that values varied across ecosystem type (ANOVA:  $F_{(5, 131)} = 14.6$ ,  $p <$   
546  $0.001$ ). The highest loss rates were observed in Yedoma and permafrost wetland ecosystems,  
547 whereas the lowest we observed in organic rich forest and permafrost bog ecosystems (Figure  
548 A4). Forest (ANOVA:  $F_{(1, 16)} = 2.31$ ,  $p = 0.15$ ) and permafrost bog (ANOVA:  $F_{(3, 24)} = 2.49$ ,  $p =$   
549  $0.09$ ) BDOC did not differ over incubation length, whereas Yedoma (ANOVA:  $F_{(4, 25)} = 24.92$ ,  $p$   
550  $< 0.001$ ) and permafrost wetland (ANOVA:  $F_{(1, 10)} = 15.87$ ,  $p < 0.01$ ) did differ over time, with  
551 their max occurring during this 40 – 90-day incubation length. This suggests that when incubated  
552 for the same number of days, we would expect greater BDOC in Yedoma and permafrost  
553 wetland ecosystems. Note, for this analysis BDOC values from all thermokarst and non-  
554 thermokarst affected sites within an ecosystem type were included.



555

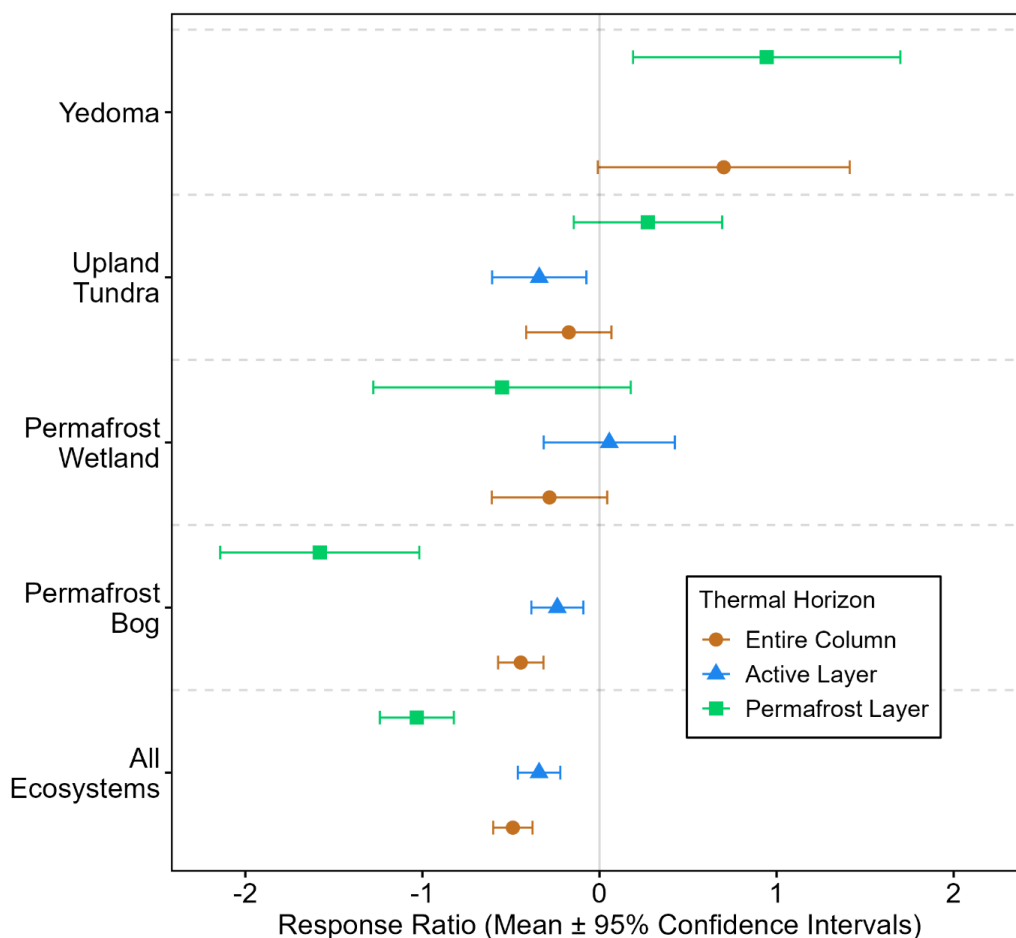
556 Figure 6. DOC concentrations ( $\text{mg L}^{-1}$ ) and biodegradable DOC (BDOC; %) from the top 3 m  
 557 following disturbance including data from both field based and incubation studies. (a) DOC  
 558 concentrations from each ecosystem type following disturbance where data was available. (b)  
 559 Biodegradable DOC (BDOC) from each ecosystem type following disturbance where data was  
 560 available. BDOC loss was determined following 3 – 304 days of incubation. Data from different  
 561 incubation lengths was combined due to low sample size. Retro Thaw Slump = Retrogressive  
 562 Thaw Slump. Boxes represents the interquartile range (25 – 75%), with median shown as black  
 563 horizontal line. Whiskers extend to 1.5 times the interquartile range (distance between first and  
 564 third quartile) in each direction, with outlier data plotted individually as black dots. Note colours  
 565 associated with boxplots in this figure are only relevant for this figure.

566 Response ratios comparing the change in DOC concentrations between pristine and  
 567 thermokarst affected sites were calculated from our dataset from 108 studies using Eq. 1 (Figure  
 568 7). Only 17 studies provided data for both pristine and thermokarst affected ecosystems, with 87  
 569 papers providing DOC concentrations from pristine and 34 from thermokarst affected sites.  
 570 When considering all ecosystems together we found that response ratios were negative,  
 571 suggesting that DOC concentrations were higher in thermokarst affected sites compared to  
 572 pristine sites (Figure 7). These negative response ratios were most evident in permafrost bogs,  
 573 where they found throughout the entire column and individual thermal horizons. The greatest



574 increase in DOC concentrations following thermokarst was seen when comparing DOC  
575 concentrations in the permafrost lens of permafrost bogs, and to a lesser extent permafrost  
576 wetlands (Figure 7). Only in Yedoma ecosystems did we see positive response ratios throughout  
577 the entire profile, suggesting a decrease in DOC concentrations following thermokarst formation  
578 in Yedoma sites. This was also seen for DOC concentrations within the permafrost lens of  
579 upland tundra sites, which include DOC concentrations from retrogressive thaw slumps and  
580 thermo-erosion gullies in their thermokarst affected sites. The large confidence intervals for  
581 some response ratios suggests high variability in the response of DOC concentrations to  
582 thermokarst formation.

583



584

585 Figure 7. Response ratios of DOC concentrations from the top 3 m following thermokarst  
586 formation (calculated using Eq. 1). Response ratio means allow for relative comparison of  
587 changes in DOC following thermokarst formation between different ecosystem types. Negative  
588 values indicate lower DOC concentrations found in pristine ecosystems, whereas positive value  
589 indicates a decrease in DOC concentrations following thermokarst. Studies reporting DOC  
590 concentrations from Exposures, Retrogressive Thaw Slumps, and Thermo-Erosion Gullies from  
591 sites within the continuous permafrost zone were combined into the Upland Tundra ecosystem  
592 category. This did not include DOC concentrations from studies within the Yedoma permafrost  
593 domain (Strauss et al., 2021). Blue line represent DOC concentrations in the active layer, as per  
594 Figure 4. Green lines represent DOC concentrations in the permafrost lens, as per Figure 4.



595 Brown lines represent DOC concentrations from the entire column (i.e., both active layer and  
596 permafrost lens).

#### 597 4. Discussion

598 In this systematic review, we evaluated patterns of DOC concentrations in the top 3 m of  
599 terrestrial ecosystems across the northern circumpolar permafrost region based on results from  
600 111 studies and 2,845 DOC measurements. We focused on comparing concentrations of DOC in  
601 soils across various geographical regions, ecological conditions, and disturbance types. Our  
602 synthesis shows that median DOC concentrations across ecosystems range from 9 – 61 mg L<sup>-1</sup>,  
603 which represents similar albeit slightly higher DOC concentrations when compared to the  
604 median DOC concentrations found in top soils of other land cover groups below 50°N (25 mg L<sup>-1</sup>  
605 <sup>-1</sup>; Langeveld et al., 2020), globally distributed lakes (6 mg L<sup>-1</sup>; Sobek et al., 2007), and lakes  
606 across the permafrost region (11 mg L<sup>-1</sup>; Stolpmann et al., 2021). In general, we show that  
607 organic soils have higher DOC concentrations than mineral soils, and that DOC concentrations  
608 are positively related to total dissolved nitrogen concentrations and negatively to C:N ratios,  
609 which corroborate previous findings of factors correlating with DOC concentrations (Aitkenhead  
610 & McDowell, 2000; Lajtha et al., 2005). Overall, we found that properties associated with  
611 ecosystem type are the main constraint on DOC concentrations. Furthermore, disturbance  
612 through permafrost thaw has little impact on measured DOC concentrations, however this may  
613 be due to the loss of biologically reactive DOC or the loss of an initially larger pulse of DOC  
614 having been previously mobilised prior to the timing of sampling.

##### 615 4.1 Environmental factors influencing DOC

616 Our database confirmed our first hypothesis that the highest DOC concentrations would be  
617 found in organic rich soils. Previous synthesis efforts estimating global distributions of terrestrial  
618 DOC concentrations have presented similar findings (Guo et al., 2020; Langeveld et al., 2020).  
619 Both of these previous studies also show that some of the highest terrestrial DOC concentrations  
620 are found within the northern circumpolar permafrost region, highlighting that these high DOC  
621 concentrations found in organic rich permafrost soils are of global significance. Concentrations  
622 of DOC in the top 3 m of soils closely mirrored stocks of SOC across the circumpolar permafrost  
623 region (Hugelius et al., 2014). Organic rich Histosol and Histel soils contain the greatest SOC



624 per km<sup>2</sup>, followed by Turbels and Orthels (Hugelius et al., 2014), as was seen in DOC  
625 concentrations across these soil types (Figure 2a). While the highest DOC concentrations are  
626 found within organic rich soils, the amount of C found as DOC represent a small amount of the  
627 total SOC pool. Using the current best estimates of Histel SOC stocks (Hugelius et al., 2020), the  
628 DOC pool represents <1% of the total C stock in permafrost-affected peatlands as has been  
629 shown for both permafrost and global soils (Guo et al., 2020; Prokushkin et al., 2008).

#### 630 *4.2 Thermal horizons*

631 In many ecosystems, DOC concentrations are greatest in the active layer nearer the  
632 surface (Figure 4). This trend has also been observed in the vertical distribution of DOC across  
633 global soils, with 50% of the DOC pool found in the top 0 – 30 cm (Guo et al., 2020). The  
634 production of DOC is associated with soil microbial activity (Guggenberger & Zech, 1993) and  
635 plant inputs (Moore & Dalva, 2001), and the microbial production of DOC via input of labile  
636 substrates has been shown to decrease with depth in permafrost (Hultman et al., 2015; Monteux  
637 et al., 2018; Wild et al., 2016). Furthermore, the organic matter content decreases and mineral  
638 content increases with depth, this depth trend and decrease in DOC with depth is particularly  
639 evident between the active layer and permafrost lens in forest ecosystems (Figure 4a). While  
640 permafrost and non-permafrost bogs do also see a shift in microbial community with depth  
641 (Heffernan & Cavaco et al., 2022; Lamit et al., 2021), the movement of modern, surface derived  
642 DOC down into deeper layers has also been observed (Chanton et al., 2008; Estop-Aragonés et  
643 al., 2018). These, combined with the large, frozen SOC stores found at depth (Hugelius et al.,  
644 2020) and hydrological isolation (Quinton, Hayashi, & Chasmer, 2011), results in a DOC pool  
645 that remains relatively similar across thermal horizons in permafrost bogs (Figure 4b).  
646 Intriguingly, in both coastal tundra and permafrost wetland ecosystems, DOC concentrations  
647 were found to be higher in the permafrost lens than in the active layer. This suggests that DOC  
648 within the active layer of these ecosystems experienced some degree of mobilization, either via  
649 export to the aquatic network or enhanced decomposition within soils. The higher DOC  
650 concentrations found within the permafrost lens of these ecosystems may represent a vulnerable  
651 DOC pool to enhanced mineralization following permafrost thaw (Figure 6).

#### 652 *4.3 Variation in DOC amongst permafrost zones and ecoregions*



653 Permafrost soils are estimated to store  $1,035 \pm 150$  Pg C globally within the top 0-3 m  
654 (Hugelius et al., 2014), with the highest storage of SOC found in the organic rich Histosols and  
655 Histels. While persistent low temperatures are the main common factor which has led to the  
656 accumulation of such high SOC amongst all permafrost soils, environmental factors associated  
657 with the different ecosystem types are the main driving factors in differences amongst DOC  
658 concentrations. The source of the permafrost DOC pool is from recent plant leachate inputs, or  
659 from the decomposition and solubilization of SOC. Thus, the molecular composition of the DOC  
660 pool is derived from a mixture of current and historical vegetation inputs. There are clear current  
661 and historical shifts in dominant vegetation seen in the permafrost region from the south (boreal)  
662 to north (arctic tundra), as well as across ecosystem types (upland forest, upland tundra, arctic  
663 and boreal wetland). However, the majority of vegetation and its leachates found in the  
664 permafrost region are generally found to produce relatively stable DOC (in terms of BDOC)  
665 consisting of lignin-derived compounds, highly aromatic polyphenolic compounds, and low  
666 molecular weight organic acids (Chen et al., 2018; Drake et al., 2015; Ewing et al., 2015; Selvam  
667 et al., 2017). While differences in the stability of different DOC source end-members have been  
668 shown (MacDonald et al., 2021), differences in redox conditions are likely a major driver in  
669 differences in the accumulation and mineralization of DOC across permafrost ecosystem types  
670 (Mohammed et al., 2022).

671 Similar to their globally significant stores of SOC (Hugelius et al., 2020), the accumulation  
672 of high DOC concentrations found in peatlands, permafrost bogs, and permafrost wetlands, is a  
673 result of the prevalence of cold and anoxic conditions throughout the Holocene (Blodau, 2002).  
674 This leads to a reduction in microbial decomposition, and the accumulation of both the SOC and  
675 DOC pool. Our results suggest that the pristine permafrost bog and permafrost wetland DOC  
676 pool is relatively stable following permafrost thaw (Figure 6, 7a). Peatland vegetation, in  
677 particular *Sphagnum* mosses, produces litter that has anti-microbial properties and is decay  
678 resistant (Hamard et al., 2019; Limpens, Bohlin, & Nilsson, 2017), limiting the amount of SOC  
679 that is degraded and assimilated into the DOC pool (Tfaily et al., 2013). This is further enhanced  
680 by the build-up of decomposition end products and the thermodynamic constraint on decay  
681 observed in anoxic soils (Beer et al., 2008). Permafrost has been continuously present in  
682 peatlands across the northern circumpolar permafrost region for the past 6,000 years, with the



683 greatest rates of permafrost formation occurring within the past 3,000 years (Treat & Jones,  
684 2018). Thus, a large proportion of the organic matter found peatlands and wetlands in this region  
685 were present prior to permafrost aggradation (i.e., permafrost formation), which indicates that  
686 permafrost formed epigenetically in these areas. Permafrost aggradation impacts soil  
687 biogeochemical properties, leading to potentially less decomposed organic matter with higher  
688 C/N ratios than non-permafrost equivalent soils, particularly in permafrost wetlands (Treat et al.,  
689 2016). This can lead to the build-up of high DOC concentrations that are vulnerable to potential  
690 mobilization following thermokarst. Decomposition in epigenetic permafrost bogs following  
691 thermokarst has been shown to be relatively slow (Heffernan et al., 2020; Manies et al., 2021),  
692 which further supports our finding (Figure 6) that the large DOC pool found in these systems in  
693 relatively stable following permafrost thaw. The permafrost wetland DOC pool that accumulates  
694 following thermokarst may represent a potentially labile DOC pool (Figure 7a), but this is likely  
695 due to fresh, plant derived inputs rather than the exposure and mineralization of previously  
696 frozen organic matter (Figure 7a).

697 Coastal tundra and forest ecosystems had similarly high DOC concentrations to those found  
698 in permafrost bogs (Figure 3a). Coastal tundra and forest ecosystems represented the highest  
699 concentrations of DOC in mineral permafrost soils. Concentrations of coastal permafrost DOC  
700 were significantly lower in the active layer compared to within the permafrost lens (Figure 4a).  
701 This is contrary to findings that deeper coastal permafrost consists of low organic matter  
702 Pleistocene marine sediments (Bristol et al., 2021) and the proximity of the active layer to  
703 vegetation inputs, although this productivity and inputs are vulnerable to projected climatic  
704 warming and regional “browning” and “greening” (Lara et al., 2018). Recent work has shown  
705 that DOC in the active layer within the coastal permafrost is more biodegradable than OC in the  
706 permafrost lens (Speetjens et al., 2022) and a substantial proportion of organic carbon derived  
707 from thawing coastal permafrost is vulnerable to mineralization upon thawing, particularly when  
708 exposed to sea water (George Tanski et al., 2021). Export of terrestrial coastal permafrost DOC  
709 directly into the Arctic Ocean can significantly influence marine biogeochemical cycles and food  
710 webs within the Arctic ocean (Bruhn et al., 2021). Arctic coasts are eroding at rates of up to 25 m  
711 yr<sup>-1</sup> (Fritz, Vonk, & Lantuit, 2017) and exporting large quantities of terrestrial organic matter  
712 export directly to the ocean that is rapidly mineralized (Tanski et al., 2019). Enhanced DOC



713 export from these coastal tundra ecosystems may disrupt aquatic food webs through altering  
714 nutrient and light supply, as has been shown for Swedish coastal systems (Peacock et al., 2022).  
715 These coastal tundra sites represent a large DOC pool that is highly vulnerable to enhanced  
716 mobilization and deserve further attention.

717 The remaining ecosystems characterised by mineral soils with an upper organic layer, i.e.,  
718 Forests, Upland Tundra, and Yedoma, followed a clear latitudinal climate gradient of increasing  
719 DOC concentrations from north to south. While not included in the most parsimonious PLS  
720 model (Figure 5), Yedoma and Upland Tundra ecosystems were found to negatively correlate  
721 with DOC concentrations (Figure A5). The greatest proportions of OC and nutrients used for  
722 DOC production are found in shallow organic layers (Semenchuk et al., 2015; Wild et al., 2013)  
723 in these ecosystems. Beneath the upper organic horizons in these mineral soils processes such as  
724 sorption of DOC to minerals and the formation of Fe-DOC or Al-DOC complexes may remove  
725 DOC from the dissolved pool (Kawahigashi et al., 2006) and mechanically protect it from  
726 mobilization (Gentsch et al., 2015). In forest ecosystems, large amounts of SOC have  
727 accumulated in surface organic layers (Hugelius et al., 2014) through increased vegetative inputs  
728 due to warmer and longer growing seasons. This organic layer depth, and the impact of soil  
729 temperature, moisture, and pH on SOC found there, strongly influences the production,  
730 concentration, and composition of DOC (Neff & Hooper, 2002; Wickland et al., 2007).  
731 Furthermore, the sorption of DOC to charcoal (Guggenberger et al., 2008), and high lignin and  
732 phenolic input from vegetation (O'Donnell et al., 2016) produce a difficult to degrade DOC pool,  
733 leading to the accumulation of the large DOC pool in this ecosystem type.

#### 734 *4.4 Vulnerability of DOC to enhanced mobilization following thermokarst*

735 We define DOC mobilization as DOC lost from an ecosystem either via export or  
736 degradation. Our second hypothesis that permafrost thaw would lead to enhanced mobilization of  
737 DOC cannot be fully supported by the findings from this database. Using our chosen systematic  
738 approach and focusing on data from terrestrial ecosystems, our database was limited to 3 studies  
739 which represented <1% of the DOC concentration data. Several previous studies have detailed  
740 the export of DOC in Arctic inland waters, see Table 2 in Ma et al., (2019), that have been  
741 excluded using this approach. We acknowledge the limitation in our approach regarding the



742 inclusion of DOC export data. Thus, this database cannot be used to determine how permafrost  
743 thaw will influence DOC export from terrestrial ecosystems within the northern circumpolar  
744 permafrost region. Currently, Arctic rivers are estimated to export 25 – 36 Tg DOC year<sup>-1</sup> (Amon  
745 et al., 2012; Holmes et al., 2012), with this being dominated by modern carbon sources (Estop-  
746 Aragonés et al., 2020), most likely derived from the top 1 m of terrestrial ecosystems. Using  
747 current best estimates of the areal extent and soil organic carbon stores in the top 1 m of  
748 Histosols, Histels, Orthels and Turbels (Hugelius et al., 2014), and if we assume that the DOC  
749 pool represents ~1% of the SOC pool, we estimate that <1% of the current DOC pool found in  
750 the top 1 m of Histosols, Histels, Orthels and Turbels is exported annually to Arctic rivers.  
751 Quantifying the proportion of these DOC pools annually lost, and particularly the proportions  
752 lost in headwater streams while being exported to Arctic rivers, is vital to assess the importance  
753 of the mobilization of the terrestrial permafrost DOC pool.

754 Our calculated response ratios (Figure 7) for all ecosystems, indicating the difference in DOC  
755 concentrations between pristine and permafrost thaw affected sites, partly supports of our second  
756 hypothesis that disturbance would lead to increased export and biodegradability of DOC. The  
757 increase in DOC following thaw observed in permafrost bogs is likely due to increased inputs  
758 due to increased runoff and shifts in vegetation following permafrost thaw (Burd, Estop-  
759 Aragonés, Tank, & Olefeldt, 2020), a relatively stable soil organic carbon pool at depth due to  
760 several millennia of microbial processing (Manies et al., 2021), the prevalence of anoxic  
761 conditions, and the potential hydrological isolation of thermokarst bogs (Quinton, Hayashi, &  
762 Pietroniro, 2003). While not included in our analysis, DOC found near the surface of the  
763 permafrost lens in forest ecosystems has been shown to be more biodegradable than DOC found  
764 in the active layer (Wickland et al., 2018), and may represent a decrease in DOC following  
765 thermokarst not captured here. Our findings of limited mobilization of permafrost bog DOC  
766 upon thawing are supported by the findings that the <sup>14</sup>C signature of DOC in Arctic rivers is  
767 dominated by modern sources (Estop-Aragonés et al., 2020). However, we do see a reduction in  
768 DOC concentrations in thermokarst affected sites at the higher latitude Yedoma upland tundra,  
769 and permafrost wetland ecosystems. This reduction in DOC concentrations in these ecosystems  
770 may be due to the greater biodegradability and lability of the DOC found there (Figure 6b),  
771 supporting our third hypothesis that the most biodegradable DOC would be found in higher



772 latitude ecosystems. Permafrost DOC in higher latitude ecosystems, particularly Yedoma  
773 ecosystems characterised by syngenetic permafrost aggradation which have not undergone  
774 centuries to millennia of soil formation and microbial processes, have been shown contain a  
775 greater proportion of low oxygen, aliphatic compounds and labile substrates (Ewing et al.,  
776 2015b; MacDonald et al., 2021). This leads to a greater biolability and rapid mineralization of  
777 DOC (Vonk et al., 2015), potentially causing the reduction in DOC concentrations observed  
778 following thaw. If this hypothesis is to be found true across all high latitude ecosystems with  
779 further data, it further highlights the vulnerability of the large DOC pool found in coastal tundra  
780 ecosystems.

781 In this study, we focus on the dissolved fraction of the OC pool, however the particulate  
782 fraction should also be considered when discussing the mobilization of terrestrial OC in  
783 permafrost landscapes. In boreal freshwater networks, particulate organic carbon (POC)  
784 represents a small but highly labile fraction of terrestrially derived OC exported to the fluvial  
785 network (Attermeyer et al., 2018). The degradation of permafrost derived POC is much slower  
786 than that of POC in the boreal freshwater network and POC derived from younger sources along  
787 the riverbank (Shakil, Tank, Kokelj, Vonk, & Zolkos, 2020). The DOC pool in Arctic  
788 freshwaters is dominated by modern terrestrial sources (Estop-Aragonés et al., 2020), whereas  
789 the POC pool has been shown to be dominated by older sources in both permafrost peatland  
790 dominated areas (Wild et al., 2019), following the formation of retrogressive thaw slumps  
791 (Keskitalo et al., 2021), and in thermokarst affected periglacial streams (Bröder et al., 2022).  
792 This older POC has been shown to accumulate following export due to low lability and  
793 degradation and mineral association, which suggests that upon thermokarst formation, previously  
794 frozen OC exported in the particulate phase is not readily consumed by microbes and that  
795 permafrost derived DOC is the more labile fraction of exported terrestrial OC.

#### 796 *4.5 Future considerations for study design*

797 Determining the fate of mobilized terrestrial DOC in both permafrost thaw affected, and  
798 pristine sites should be prioritized in future studies to constrain current estimates of the  
799 permafrost C climate feedback. There are large spatial gaps in the database, particularly in areas  
800 with large stock of permafrost C such as the Hudson Bay Lowlands and Mackenzie River Basin,



801 both in Canada and two of the three largest deposits of permafrost peatland C in the circumpolar  
802 permafrost region (Olefeldt et al., 2021). Similarly, coastal tundra sites, which along with  
803 permafrost bog represent the ecosystems with the highest DOC concentrations, were sampled  
804 only along the northern shoreline of Alaska and the Yukon (USA and Canada, respectively;  
805 Table S1). From our analysis of this database, we determine that DOC mobilization is poorly  
806 understood for terrestrial permafrost ecosystems. To address this, the two main needs of future  
807 studies are 1) more direct estimates of DOC fluxes and export from terrestrial ecosystems into  
808 aquatic ecosystems, and 2) more DOC degradation (BDOC) and mineralization studies. Our  
809 results suggest that the high concentrations of DOC in permafrost bogs remains relatively stable  
810 upon thermokarst formation, although individual studies do indicate that thawing peat may  
811 provide a reactive source of DOC (Panneer Selvam et al., 2017). Whereas the database did not  
812 include any studies that reported on the mineralization of DOC from coastal tundra sites. Further  
813 sampling and assessing the mineralization of DOC is required to characterize the potential pool  
814 of vulnerable DOC in areas with high DOC concentrations. Overall, our database and systematic  
815 approach only included 5 studies (Olefeldt & Roulet, 2012, 2014; Olefeldt et al., 2012;  
816 Prokushkin et al., 2006; Prokushkin et al., 2005) that explicitly reported rates of DOC discharge,  
817 export, or fluxes from terrestrial ecosystems into the fluvial network. Given the importance of  
818 terrestrial DOC as a source for CO<sub>2</sub> production within the aquatic network (Weyhenmeyer et al.,  
819 2012), and the findings that previously frozen DOC is being exported to the freshwater network  
820 (Estop-Aragones et al., 2020), improved estimates of the quantity of terrestrial DOC being  
821 exported is essential to determine the potential aquatic greenhouse gas fluxes derived from the  
822 mineralization of terrigenous organic matter. To improve current estimates of the permafrost C  
823 feedback further studies are needed to determine how much DOC is laterally exported from  
824 terrestrial ecosystems, and the mineralization potential of this DOC along the terrestrial-  
825 freshwater-aquatic continuum.

826 Lastly, we suggest that future studies should consider a standardization of methods and  
827 approaches used to determine DOC concentrations for better comparison across studies. In  
828 constructing this database we identified 3 different filter sizes, 11 different extraction procedures,  
829 and 4 different measurement methods. The most common filter size used was 0.45 µm and this  
830 has previously been described as the cut off to separate DOC from colloid materials (Thurman



831 1985; Bolan et al., 1999). In extracting DOC concentrations from soils the mostly commonly  
832 used approach (70% of all soil samples) was via soil leaching with no chemical treatment of the  
833 soils, although some added filtered water to promote leaching. From the seven approaches  
834 identified to extract water samples from terrestrial sites in determining DOC, 48% of samples  
835 were collected using a variety of suction devices and 46% done via grab samples. Of the four  
836 DOC measurements methods the most common approach was by combustion, with 90% of all  
837 DOC concentrations measured using this approach. As such, in order to continue measuring  
838 DOC concentrations in terrestrial permafrost ecosystems using the most consistent approach we  
839 suggest using 0.45  $\mu\text{m}$  filters, extracting pore water via some type of sucking device or soils via  
840 leaching, and using a combustion based method to determine DOC concentrations

#### 841 **Data availability**

842 All data will be made freely and publicly available on an online repository prior to publication

#### 843 **Author contributions**

844 LH, DK, and LT designed and planned the systematic review approach; LH built the database.  
845 LH and DK analyzed the data; LH wrote the manuscript draft; DK and LT edited and reviewed  
846 the manuscript.

#### 847 **Competing interests**

848 The authors declare that they have no conflict of interest.

#### 849 **Acknowledgements**

850 We thank Konstantinos Vaziourakis, Mona Abbasi, Elizabeth Jakobsson, Marloes Groeneveld,  
851 Sarah Shakil, and Jeffrey Hawkes for helpful discussions throughout the development and  
852 writing of this manuscript.

#### 853 **Financial support**

854 This work was supported by the Knut and Alice Wallenberg Foundation.



855 **References (in text)**

- 856 Aitkenhead, J. A., & McDowell, W. H. (2000). Soil C:N ratio as a predictor of annual riverine  
857 DOC flux at local and global scales. *Global Biogeochemical Cycles*, 14(1).  
858 <https://doi.org/10.1029/1999GB900083>
- 859 Amon, R. M. W., Rinehart, A. J., Duan, S., Louchouart, P., Prokushkin, A., Guggenberger, G.,  
860 ... Zhulidov, A. V. (2012). Dissolved organic matter sources in large Arctic rivers.  
861 *Geochimica et Cosmochimica Acta*, 94, 217–237.  
862 <https://doi.org/https://doi.org/10.1016/j.gca.2012.07.015>
- 863 Arksey, H., & O'Malley, L. (2005). Scoping studies: Towards a methodological framework.  
864 *International Journal of Social Research Methodology: Theory and Practice*, 8(1).  
865 <https://doi.org/10.1080/1364557032000119616>
- 866 Attermeyer, K., Catalán, N., Einarsdottir, K., Freixa, A., Groeneveld, M., Hawkes, J. A., ...  
867 Tranvik, L. J. (2018). Organic Carbon Processing During Transport Through Boreal Inland  
868 Waters: Particles as Important Sites. *Journal of Geophysical Research: Biogeosciences*,  
869 123(8). <https://doi.org/10.1029/2018JG004500>
- 870 Beckebanze, L., Runkle, B. R. K., Walz, J., Wille, C., Holl, D., Helbig, M., ... Kutzbach, L.  
871 (2022). Lateral carbon export has low impact on the net ecosystem carbon balance of a  
872 polygonal tundra catchment. *BIOGEOSCIENCES*, 19(16), 3863–3876.  
873 <https://doi.org/10.5194/bg-19-3863-2022>
- 874 Beer, J., Lee, K., Whittier, M., & Blodau, C. (2008). Geochemical controls on anaerobic organic  
875 matter decomposition in a northern peatland. *Limnology and Oceanography*, 53(4), 1393–  
876 1407. <https://doi.org/10.4319/lo.2008.53.4.1393>
- 877 Biester, H., Knorr, K. H., Schellekens, J., Basler, A., & Hermanns, Y. M. (2014). Comparison of  
878 different methods to determine the degree of peat decomposition in peat bogs.  
879 *Biogeosciences*. <https://doi.org/10.5194/bg-11-2691-2014>
- 880 Blodau, C. (2002). Carbon cycling in peatlands &#151; A review of processes and controls.  
881 *Environmental Reviews*, 10(2), 111–134. <https://doi.org/10.1139/a02-004>
- 882 Bolan, N.S., Baskaran, S., Thiagarajan, S. (1999). Methods of Measurement of Dissolved  
883 Organic Carbon of Plant Origin in Soils, Manures, Sludges and Stream Water. In: Linskens,  
884 H.F., Jackson, J.F. (eds) *Analysis of Plant Waste Materials. Modern Methods of Plant*  
885 *Analysis*, vol 20. Springer, Berlin, Heidelberg. [https://doi.org/10.1007/978-3-662-03887-1\\_1](https://doi.org/10.1007/978-3-662-03887-1_1)  
886
- 887 Bristol, E. M., Connolly, C. T., Lorenson, T. D., Richmond, B. M., Ilgen, A. G., Choens, R. C.,  
888 ... McClelland, J. W. (2021). Geochemistry of Coastal Permafrost and Erosion-Driven  
889 Organic Matter Fluxes to the Beaufort Sea Near Drew Point, Alaska. *Frontiers in Earth*  
890 *Science*, 8. <https://doi.org/10.3389/feart.2020.598933>



- 891 Bröder, L., Hirst, C., Opfergelt, S., Thomas, M., Vonk, J. E., Haghypour, N., ... Fouché, J.  
892 (2022). Contrasting Export of Particulate Organic Carbon From Greenlandic Glacial and  
893 Nonglacial Streams. *Geophysical Research Letters*, 49(21).  
894 <https://doi.org/10.1029/2022GL101210>
- 895 Brown, J., Ferrians Jr., O. J., Heginbottom, J. A., & Melnikov, E. S. (1997). Circum-Arctic map  
896 of permafrost and ground ice conditions. *USGS Numbered Series*, 1.  
897 <https://doi.org/10.1016/j.jallcom.2010.03.054>
- 898 Bruhn, A. D., Stedmon, C. A., Comte, J., Matsuoka, A., Speetjens, N. J., Tanski, G., ... Sjöstedt,  
899 J. (2021). Terrestrial Dissolved Organic Matter Mobilized From Eroding Permafrost  
900 Controls Microbial Community Composition and Growth in Arctic Coastal Zones.  
901 *Frontiers in Earth Science*, 9. <https://doi.org/10.3389/feart.2021.640580>
- 902 Burd, K., Estop-Aragonés, C., Tank, S. E., & Olefeldt, D. (2020). Lability of dissolved organic  
903 carbon from boreal peatlands: interactions between permafrost thaw, wildfire, and season.  
904 *Canadian Journal of Soil Science*, 13(February), 1–13. <https://doi.org/10.1139/cjss-2019-0154>  
905
- 906 Camill, P. (2005). Permafrost thaw accelerates in boreal peatlands during late-20th century  
907 climate warming. *Climatic Change*, 68(1–2), 135–152. <https://doi.org/10.1007/s10584-005-4785-y>  
908
- 909 Chanton, J. P., Glaser, P. H., Chasar, L. S., Burdige, D. J., Hines, M. E., Siegel, D. I., ... Cooper,  
910 W. T. (2008). Radiocarbon evidence for the importance of surface vegetation on  
911 fermentation and methanogenesis in contrasting types of boreal peatlands. *Global*  
912 *Biogeochemical Cycles*, 22(4), 1–11. <https://doi.org/10.1029/2008GB003274>
- 913 Chen, H., Yang, Z., Chu, R. K., Tolic, N., Liang, L., Graham, D. E., ... Gu, B. (2018). Molecular  
914 Insights into Arctic Soil Organic Matter Degradation under Warming. *ENVIRONMENTAL*  
915 *SCIENCE & TECHNOLOGY*, 52(8), 4555–4564. <https://doi.org/10.1021/acs.est.7b05469>
- 916 Connon, R. F., Quinton, W. L., Craig, J. R., & Hayashi, M. (2014). Changing hydrologic  
917 connectivity due to permafrost thaw in the lower Liard River valley, NWT, Canada.  
918 *Hydrological Processes*, 28(14). <https://doi.org/10.1002/hyp.10206>
- 919 Dean, J. F., Meisel, O. H., Rosco, M. M., Marchesini, L. B., Garnett, M. H., Lenderink, H., ...  
920 Dolman, A. J. (2020). East Siberian Arctic inland waters emit mostly contemporary carbon.  
921 *NATURE COMMUNICATIONS*, 11(1). <https://doi.org/10.1038/s41467-020-15511-6>
- 922 Drake, T. W., Wickland, K. P., Spencer, R. G. M., McKnight, D. M., & Striegl, R. G. (2015).  
923 Ancient low-molecular-weight organic acids in permafrost fuel rapid carbon dioxide  
924 production upon thaw. *PROCEEDINGS OF THE NATIONAL ACADEMY OF SCIENCES*  
925 *OF THE UNITED STATES OF AMERICA*, 112(45), 13946–13951.  
926 <https://doi.org/10.1073/pnas.1511705112>



- 927 Estop-Aragones, C., Olefeldt, D., Abbott, B. W., Chanton, J. P., Czimczik, C. I., Dean, J. F., ...  
928 Anthony, K. W. (2020). Assessing the Potential for Mobilization of Old Soil Carbon After  
929 Permafrost Thaw: A Synthesis of C-14 Measurements From the Northern Permafrost  
930 Region. *GLOBAL BIOGEOCHEMICAL CYCLES*, 34(9).  
931 <https://doi.org/10.1029/2020GB006672>
- 932 Estop-Aragones, Cristian, Czimczik, C. I., Heffernan, L., Gibson, C., Walker, J. C., Xu, X., &  
933 Olefeldt, D. (2018). Respiration of aged soil carbon during fall in permafrost peatlands  
934 enhanced by active layer deepening following wildfire but limited following thermokarst.  
935 *Environmental Research Letters*, 13(8). <https://doi.org/10.1088/1748-9326/aad5f0>
- 936 Ewing, S. A., Paces, J. B., O'Donnell, J. A., Jorgenson, M. T., Kanevskiy, M. Z., Aiken, G. R.,  
937 ... Striegl, R. (2015a). Uranium isotopes and dissolved organic carbon in loess permafrost:  
938 Modeling the age of ancient ice. *GEOCHIMICA ET COSMOCHIMICA ACTA*, 152, 143–  
939 165. <https://doi.org/10.1016/j.gca.2014.11.008>
- 940 Ewing, S. A., Paces, J. B., O'Donnell, J. A., Jorgenson, M. T., Kanevskiy, M. Z., Aiken, G. R.,  
941 ... Striegl, R. (2015b). Uranium isotopes and dissolved organic carbon in loess permafrost:  
942 Modeling the age of ancient ice. *Geochimica et Cosmochimica Acta*, 152, 143–165.  
943 <https://doi.org/10.1016/j.gca.2014.11.008>
- 944 Fritz, M., Vonk, J. E., & Lantuit, H. (2017). Collapsing Arctic coastlines. *Nature Climate*  
945 *Change*. <https://doi.org/10.1038/nclimate3188>
- 946 Gentsch, N., Mikutta, R., Shibistova, O., Wild, B., Schnecker, J., Richter, A., ... Guggenberger,  
947 G. (2015). Properties and bioavailability of particulate and mineral-associated organic  
948 matter in Arctic permafrost soils, Lower Kolyma Region, Russia. *European Journal of Soil*  
949 *Science*, 66(4). <https://doi.org/10.1111/ejss.12269>
- 950 Guggenberger, G., & Zech, W. (1993). Dissolved organic carbon control in acid forest soils of  
951 the Fichtelgebirge (Germany) as revealed by distribution patterns and structural  
952 composition analyses. *Geoderma*, 59(1–4). [https://doi.org/10.1016/0016-7061\(93\)90065-S](https://doi.org/10.1016/0016-7061(93)90065-S)
- 953 Guggenberger, Georg, Rodionov, A., Shibistova, O., Grabe, M., Kasansky, O. A., Fuchs, H., ...  
954 Flessa, H. (2008). Storage and mobility of black carbon in permafrost soils of the forest  
955 tundra ecotone in Northern Siberia. *Global Change Biology*, 14(6), 1367–1381.  
956 <https://doi.org/10.1111/j.1365-2486.2008.01568.x>
- 957 Guo, Z., Wang, Y., Wan, Z., Zuo, Y., He, L., Li, D., ... Xu, X. (2020). Soil dissolved organic  
958 carbon in terrestrial ecosystems: Global budget, spatial distribution and controls. *Global*  
959 *Ecology and Biogeography*, 29(12). <https://doi.org/10.1111/geb.13186>
- 960 Hamard, S., Robroek, B. J. M., Allard, P. M., Signarbieux, C., Zhou, S., Saesong, T., ... Jassey,  
961 V. E. J. (2019). Effects of Sphagnum Leachate on Competitive Sphagnum Microbiome  
962 Depend on Species and Time. *Frontiers in Microbiology*, 10.  
963 <https://doi.org/10.3389/fmicb.2019.02042>



- 964 Hansen, A. M., Kraus, T. E. C., Pellerin, B. A., Fleck, J. A., Downing, B. D., & Bergamaschi, B.  
965 A. (2016). Optical properties of dissolved organic matter (DOM): Effects of biological and  
966 photolytic degradation. *Limnology and Oceanography*, **61**(3), 1015–  
967 1032. <https://doi.org/10.1002/lno.10270>
- 968 Heffernan, L., Cavaco, M. A., Bhatia, M. P., Estop-Aragonés, C., Knorr, K.-H., & Olefeldt, D.  
969 (2022). High peatland methane emissions following permafrost thaw: enhanced acetoclastic  
970 methanogenesis during early successional stages. *Biogeosciences*, *19*(12).  
971 <https://doi.org/10.5194/bg-19-3051-2022>
- 972 Heffernan, L., Estop-Aragonés, C., Knorr, K.-H., Talbot, J., & Olefeldt, D. (2020). Long-term  
973 impacts of permafrost thaw on carbon storage in peatlands: deep losses offset by surficial  
974 accumulation. *Journal of Geophysical Research: Biogeosciences*, *2011*(2865),  
975 e2019JG005501. <https://doi.org/10.1029/2019JG005501>
- 976 Holmes, R. M., McClelland, J. W., Peterson, B. J., Tank, S. E., Bulygina, E., Eglinton, T. I., ...  
977 Zimov, S. A. (2012). Seasonal and Annual Fluxes of Nutrients and Organic Matter from  
978 Large Rivers to the Arctic Ocean and Surrounding Seas. *ESTUARIES AND COASTS*, *35*(2),  
979 369–382. <https://doi.org/10.1007/s12237-011-9386-6>
- 980 Hugelius, G., Strauss, J., Zubrzycki, S., Harden, J. W., Schuur, E. A. G., Ping, C. L., ... Kuhry,  
981 P. (2014). Estimated stocks of circumpolar permafrost carbon with quantified uncertainty  
982 ranges and identified data gaps. *Biogeosciences*, *11*(23), 6573–6593.  
983 <https://doi.org/10.5194/bg-11-6573-2014>
- 984 Hugelius, Gustaf, Loisel, J., Chadburn, S., Jackson, R. B., Jones, M., MacDonald, G., ... Yu, Z.  
985 (2020). Large stocks of peatland carbon and nitrogen are vulnerable to permafrost thaw.  
986 *Proceedings of the National Academy of Sciences*, *117*(34), 20438–20446.  
987 <https://doi.org/10.1073/pnas.1916387117>
- 988 Hultman, J., Waldrop, M. P., Mackelprang, R., David, M. M., McFarland, J., Blazewicz, S. J., ...  
989 Jansson, J. K. (2015). Multi-omics of permafrost, active layer and thermokarst bog soil  
990 microbiomes. *Nature*, *521*(7551). <https://doi.org/10.1038/nature14238>
- 991 Jorgenson, M. T., Shur, Y. L., & Pullman, E. R. (2006). Abrupt increase in permafrost  
992 degradation in Arctic Alaska. *Geophysical Research Letters*, *33*(2).  
993 <https://doi.org/10.1029/2005GL024960>
- 994 Kawahigashi, M., Kaiser, K., Rodionov, A., & Guggenberger, G. (2006). Sorption of dissolved  
995 organic matter by mineral soils of the Siberian forest tundra. *GLOBAL CHANGE*  
996 *BIOLOGY*, *12*(10), 1868–1877. <https://doi.org/10.1111/j.1365-2486.2006.01203.x>
- 997 Keskitalo, K. H., Bröder, L., Shakil, S., Zolkos, S., Tank, S. E., van Dongen, B. E., ... Vonk, J.  
998 E. (2021). Downstream Evolution of Particulate Organic Matter Composition From  
999 Permafrost Thaw Slumps. *Frontiers in Earth Science*, *9*.  
1000 <https://doi.org/10.3389/feart.2021.642675>



- 1001 Kicklighter, D. W., Hayes, D. J., McClelland, J. W., Peterson, B. J., McGuire, A. D., & Melillo,  
1002 J. M. (2013). Insights and issues with simulating terrestrial DOC loading of Arctic river  
1003 networks. *ECOLOGICAL APPLICATIONS*, 23(8), 1817–1836. <https://doi.org/10.1890/11-1050.1>  
1004
- 1005 Kokelj, S. V., & Jorgenson, M. T. (2013). Advances in thermokarst research. *Permafrost and*  
1006 *Periglacial Processes*, 24(2), 108–119. <https://doi.org/10.1002/ppp.1779>
- 1007 Lajeunesse, M. J. (2011). On the meta-analysis of response ratios for studies with correlated and  
1008 multi-group designs. *Ecology*, 92(11). <https://doi.org/10.1890/11-0423.1>
- 1009 Lajtha, K., Crow, S. E., Yano, Y., Kaushal, S. S., Sulzman, E., Sollins, P., & Spears, J. D. H.  
1010 (2005). Detrital controls on soil solution N and dissolved organic matter in soils: A field  
1011 experiment. *Biogeochemistry*, 76(2). <https://doi.org/10.1007/s10533-005-5071-9>
- 1012 Lamit, L. J., Romanowicz, K. J., Potvin, L. R., Lennon, J. T., Tringe, S. G., Chimner, R. A., ...  
1013 Lilleskov, E. A. (2021). Peatland microbial community responses to plant functional group  
1014 and drought are depth-dependent. *Molecular Ecology*, 30(20).  
1015 <https://doi.org/10.1111/mec.16125>
- 1016 Langeveld, J., Bouwman, A. F., van Hoek, W. J., Vilmin, L., Beusen, A. H. W., Mogollón, J. M.,  
1017 & Middelburg, J. J. (2020). Estimating dissolved carbon concentrations in global soils: a  
1018 global database and model. *SN Applied Sciences*, 2(10), 1–21.  
1019 <https://doi.org/10.1007/s42452-020-03290-0>
- 1020 Lara, M. J., Nitze, I., Grosse, G., Martin, P., & David McGuire, A. (2018). Reduced arctic tundra  
1021 productivity linked with landform and climate change interactions. *Scientific Reports*, 8(1).  
1022 <https://doi.org/10.1038/s41598-018-20692-8>
- 1023 Liljedahl, A. K., Boike, J., Daanen, R. P., Fedorov, A. N., Frost, G. V., Grosse, G., ... Zona, D.  
1024 (2016). Pan-Arctic ice-wedge degradation in warming permafrost and its influence on  
1025 tundra hydrology. *Nature Geoscience*, 9(4). <https://doi.org/10.1038/ngeo2674>
- 1026 Limpens, J., Bohlin, E., & Nilsson, M. B. (2017). Phylogenetic or environmental control on the  
1027 elemental and organo-chemical composition of Sphagnum mosses? *Plant and Soil*.  
1028 <https://doi.org/10.1007/s11104-017-3239-4>
- 1029 Ma, Q., Jin, H., Yu, C., & Bense, V. F. (2019). Dissolved organic carbon in permafrost regions:  
1030 A review. *Science China Earth Sciences*. <https://doi.org/10.1007/s11430-018-9309-6>
- 1031 MacDonald, E. N., Tank, S. E., Kokelj, S. V., Froese, D. G., & Hutchins, R. H. S. (2021).  
1032 Permafrost-derived dissolved organic matter composition varies across permafrost end-  
1033 members in the western Canadian Arctic. *Environmental Research Letters*, 16(2).  
1034 <https://doi.org/10.1088/1748-9326/abd971>
- 1035 Manies, K. L., Jones, M. C., Waldrop, M. P., Leewis, M. C., Fuller, C., Cornman, R. S., &



- 1036 Hoefke, K. (2021). Influence of Permafrost Type and Site History on Losses of Permafrost  
1037 Carbon After Thaw. *Journal of Geophysical Research: Biogeosciences*, 126(11).  
1038 <https://doi.org/10.1029/2021JG006396>
- 1039 McGuire, A. D., Lawrence, D. M., Koven, C., Klein, J. S., Burke, E., Chen, G., ... Zhuang, Q.  
1040 (2018). Dependence of the evolution of carbon dynamics in the northern permafrost region  
1041 on the trajectory of climate change. *Proceedings of the National Academy of Sciences of the*  
1042 *United States of America*, 115(15). <https://doi.org/10.1073/pnas.1719903115>
- 1043 Mehmood, T., Liland, K. H., Snipen, L., & Sæbø, S. (2012). A review of variable selection  
1044 methods in Partial Least Squares Regression. *Chemometrics and Intelligent Laboratory*  
1045 *Systems*. <https://doi.org/10.1016/j.chemolab.2012.07.010>
- 1046 Mevik, B. H., & Wehrens, R. (2007). The pls package: Principal component and partial least  
1047 squares regression in R. *Journal of Statistical Software*, 18(2).  
1048 <https://doi.org/10.18637/jss.v018.i02>
- 1049 Miner, K. R., Turetsky, M. R., Malina, E., Bartsch, A., Tamminen, J., McGuire, A. D., ... Miller,  
1050 C. E. (2022). Permafrost carbon emissions in a changing Arctic. *Nature Reviews Earth and*  
1051 *Environment*. <https://doi.org/10.1038/s43017-021-00230-3>
- 1052 Mohammed, A. A., Guimond, J. A., Bense, V. F., Jamieson, R. C., McKenzie, J. M., & Kurylyk,  
1053 B. L. (2022). Mobilization of subsurface carbon pools driven by permafrost thaw and  
1054 reactivation of groundwater flow: a virtual experiment. *Environmental Research Letters*,  
1055 17(12), 124036. <https://doi.org/10.1088/1748-9326/ACA701>
- 1056 Monteux, S., Weedon, J. T., Blume-Werry, G., Gavazov, K., Jassey, V. E. J., Johansson, M., ...  
1057 Dorrepaal, E. (2018). Long-term in situ permafrost thaw effects on bacterial communities  
1058 and potential aerobic respiration. *ISME Journal*, 12(9), 2129–2141.  
1059 <https://doi.org/10.1038/s41396-018-0176-z>
- 1060 Moore, T. R., & Dalva, M. (2001). Some controls on the release of dissolved organic carbon by  
1061 plant tissues and soils. *Soil Science*, 166(1), 38–47. [https://doi.org/10.1097/00010694-](https://doi.org/10.1097/00010694-200101000-00007)  
1062 [200101000-00007](https://doi.org/10.1097/00010694-200101000-00007)
- 1063 Neff, J. C., & Hooper, D. U. (2002). Vegetation and climate controls on potential CO<sub>2</sub>, DOC and  
1064 DON production in northern latitude soils. *Global Change Biology*, 8(9), 872–884.  
1065 <https://doi.org/10.1046/j.1365-2486.2002.00517.x>
- 1066 O'Donnell, J. A., Aiken, G. R., Butler, K. D., Guillemette, F., Podgorski, D. C., & Spencer, R.  
1067 G. M. (2016). DOM composition and transformation in boreal forest soils: The effects of  
1068 temperature and organic-horizon decomposition state. *Journal of Geophysical Research:*  
1069 *Biogeosciences*, 121(10), 2727–2744. <https://doi.org/10.1002/2016JG003431>.Received
- 1070 Olefeldt, D., Heffernan, L., Jones, M. C., Sannel, A. B. K., Treat, C. C., & Turetsky, M. R.  
1071 (2021). Permafrost Thaw in Northern Peatlands: Rapid Changes in Ecosystem and



- 1072 Landscape Functions (pp. 27–67). [https://doi.org/10.1007/978-3-030-71330-0\\_3](https://doi.org/10.1007/978-3-030-71330-0_3)
- 1073 Olefeldt, D., & Roulet, N. T. (2012). Effects of permafrost and hydrology on the composition  
1074 and transport of dissolved organic carbon in a subarctic peatland complex. *Journal of*  
1075 *Geophysical Research: Biogeosciences*, 117(1). <https://doi.org/10.1029/2011JG001819>
- 1076 Olefeldt, D., & Roulet, N. T. (2014). Permafrost conditions in peatlands regulate magnitude,  
1077 timing, and chemical composition of catchment dissolved organic carbon export. *GLOBAL*  
1078 *CHANGE BIOLOGY*, 20(10), 3122–3136. <https://doi.org/10.1111/gcb.12607>
- 1079 Olefeldt, D., Roulet, N. T., Bergeron, O., Crill, P., Bäckstrand, K., & Christensen, T. R. (2012).  
1080 Net carbon accumulation of a high-latitude permafrost palsa mire similar to permafrost-free  
1081 peatlands. *Geophysical Research Letters*, 39(3). <https://doi.org/10.1029/2011GL050355>
- 1082 Olson, D. M., Dinerstein, E., Wikramanayake, E. D., Burgess, N. D., Powell, G. V. N.,  
1083 Underwood, E. C., ... others. (2001). Terrestrial Ecoregions of the World: A New Map of  
1084 Life on Earth: A new global map of terrestrial ecoregions provides an innovative tool for  
1085 conserving biodiversity. *BioScience*, 51(11).
- 1086 Panneer Selvam, B., Lapierre, J.-F., Guillemette, F., Voigt, C., Lamprecht, R. E., Biasi, C., ...  
1087 Berggren, M. (2017). Degradation potentials of dissolved organic carbon (DOC) from  
1088 thawed permafrost peat. *SCIENTIFIC REPORTS*, 7, 45811.  
1089 <https://doi.org/10.1038/srep45811>
- 1090 Peacock, M., Futter, M. N., Jutterström, S., Kothawala, D. N., Moldan, F., Stadmark, J., &  
1091 Evans, C. D. (2022). Three Decades of Changing Nutrient Stoichiometry from Source to  
1092 Sea on the Swedish West Coast. *Ecosystems*, 25(8). <https://doi.org/10.1007/s10021-022-00798-x>  
1093
- 1094 Pries, C. E. H., Schuur, E. A. G., & Crummer, K. G. (2012). Holocene Carbon Stocks and  
1095 Carbon Accumulation Rates Altered in Soils Undergoing Permafrost Thaw. *Ecosystems*,  
1096 15(1). <https://doi.org/10.1007/s10021-011-9500-4>
- 1097 Prokushkin, A. S., Gavrilenko, I. V., Abaimov, A. P., Prokushkin, S. G., & Samusenko, A. V.  
1098 (2006). Dissolved organic carbon in upland forested watersheds underlain by continuous  
1099 permafrost in Central Siberia. *Mitigation and Adaptation Strategies for Global Change*,  
1100 11(1), 223–240. <https://doi.org/10.1007/s11027-006-1022-6>
- 1101 Prokushkin, A S, Kajimoto, T., Prokushkin, S. G., McDowell, W. H., Abaimov, A. P., &  
1102 Matsuura, Y. (2005). Climatic factors influencing fluxes of dissolved organic carbon from  
1103 the forest floor in a continuous-permafrost Siberian watershed. *CANADIAN JOURNAL OF*  
1104 *FOREST RESEARCH*, 35(9), 2130–2140. <https://doi.org/10.1139/X05-150>
- 1105 Prokushkin, Anatoly S., Kawahigashi, M., & Tokareva, I. V. (2008). Global Warming and  
1106 Dissolved Organic Carbon Release from Permafrost Soils. In *Permafrost Soils* (pp. 237–  
1107 250). [https://doi.org/10.1007/978-3-540-69371-0\\_16](https://doi.org/10.1007/978-3-540-69371-0_16)



- 1108 Quinton, W. L., Hayashi, M., & Chasmer, L. E. (2011). Permafrost-thaw-induced land-cover  
1109 change in the Canadian subarctic: Implications for water resources. *Hydrological Processes*,  
1110 25(1), 152–158. <https://doi.org/10.1002/hyp.7894>
- 1111 Quinton, W. L., Hayashi, M., & Pietroniro, A. (2003). Connectivity and storage functions of  
1112 channel fens and flat bogs in northern basins. *Hydrological Processes*.  
1113 <https://doi.org/10.1002/hyp.1369>
- 1114 Rantanen, M., Karpechko, A., Lipponen, A., Nordling, K., Hyvärinen, O., Ruosteenoja, K., ...  
1115 Laaksonen, A. (2021). The Arctic has warmed four times faster than the globe since 1980.  
1116 *Nature Portfolio*, (2022), 0–29. <https://doi.org/https://doi.org/10.1038/s43247-022-00498-3>
- 1117 Raymond, P. A., McClelland, J. W., Holmes, R. M., Zhulidov, A. V., Mull, K., Peterson, B. J.,  
1118 ... Gurtovaya, T. Y. (2007). Flux and age of dissolved organic carbon exported to the Arctic  
1119 Ocean: A carbon isotopic study of the five largest arctic rivers. *Global Biogeochemical*  
1120 *Cycles*, 21(4). <https://doi.org/10.1029/2007GB002934>
- 1121 Ripley, B., Venables, B., Bates, D. M., Hornik, K., Gebhardt, A., & Firth, D. (2019). Package  
1122 ‘MASS’ (Version 7.3-51.4). *Cran-R Project*.
- 1123 Schaefer, K., Lantuit, H., Romanovsky, V. E., Schuur, E. A. G., & Witt, R. (2014). The impact  
1124 of the permafrost carbon feedback on global climate. *Environmental Research Letters*.  
1125 <https://doi.org/10.1088/1748-9326/9/8/085003>
- 1126 Schuur, E. A. G., Bracho, R., Celis, G., Belshe, E. F., Ebert, C., Ledman, J., ... Webb, E. E.  
1127 (2021). Tundra Underlain By Thawing Permafrost Persistently Emits Carbon to the  
1128 Atmosphere Over 15 Years of Measurements. *Journal of Geophysical Research:*  
1129 *Biogeosciences*, 126(6), 1–23. <https://doi.org/10.1029/2020jg006044>
- 1130 Schuur, T., McGuire, A. D., Romanovsky, V., Schädel, C., & Mack, M. (2018). Chapter 11:  
1131 Arctic and Boreal Carbon. Second State of the Carbon Cycle Report. *Second State of the*  
1132 *Carbon Cycle Report (SOCCR2): A Sustained Assessment Report*, 428–468. Retrieved from  
1133 <https://carbon2018.globalchange.gov/chapter/11/>
- 1134 Selvam, B. P., Lapierre, J.-F., Guillemette, F., Voigt, C., Lamprecht, R. E., Biasi, C., ...  
1135 Berggren, M. (2017). Degradation potentials of dissolved organic carbon (DOC) from  
1136 thawed permafrost peat. *SCIENTIFIC REPORTS*, 7. <https://doi.org/10.1038/srep45811>
- 1137 Semenchuk, P. R., Elberling, B., Amtorp, C., Winkler, J., Rumpf, S., Michelsen, A., & Cooper,  
1138 E. J. (2015). Deeper snow alters soil nutrient availability and leaf nutrient status in high  
1139 Arctic tundra. *Biogeochemistry*, 124(1–3), 81–94. <https://doi.org/10.1007/s10533-015-0082-7>
- 1141 Shakil, S., Tank, S. E., Kokelj, S. V., Vonk, J. E., & Zolkos, S. (2020). Particulate dominance of  
1142 organic carbon mobilization from thaw slumps on the Peel Plateau, NT: Quantification and  
1143 implications for stream systems and permafrost carbon release. *Environmental Research*



- 1144 *Letters*, 15(11). <https://doi.org/10.1088/1748-9326/abac36>
- 1145 Sobek, S., Tranvik, L. J., Prairie, Y. T., Kortelainen, P., & Cole, J. J. (2007). Patterns and  
1146 regulation of dissolved organic carbon: An analysis of 7,500 widely distributed lakes.  
1147 *Limnology and Oceanography*, 52(3). <https://doi.org/10.4319/lo.2007.52.3.1208>
- 1148 Speetjens, N. J., Tanski, G., Martin, V., Wagner, J., Richter, A., Hugelius, G., ... Vonk, J. E.  
1149 (2022). Dissolved organic matter characterization in soils and streams in a small coastal  
1150 low-arctic catchment. *Biogeosciences*, 19(July), 3073–3097. Retrieved from  
1151 <https://doi.org/10.5194/bg-19-3073-2022>
- 1152 Stolpmann, L., Coch, C., Morgenstern, A., Boike, J., Fritz, M., Herzsuh, U., ... Grosse, G.  
1153 (2021). First pan-Arctic assessment of dissolved organic carbon in lakes of the permafrost  
1154 region. *BIOGEOSCIENCES*, 18(12), 3917–3936. <https://doi.org/10.5194/bg-18-3917-2021>
- 1155 Strauss, J., Laboor, S., Schirrmeister, L., Fedorov, A. N., Fortier, D., Froese, D., ... Grosse, G.  
1156 (2021). Circum-Arctic Map of the Yedoma Permafrost Domain. *Frontiers in Earth Science*,  
1157 9. <https://doi.org/10.3389/feart.2021.758360>
- 1158 Striegl, R. G., Aiken, G. R., Dornblaser, M. M., Raymond, P. A., & Wickland, K. P. (2005). A  
1159 decrease in discharge-normalized DOC export by the Yukon River during summer through  
1160 autumn. *GEOPHYSICAL RESEARCH LETTERS*, 32(21).  
1161 <https://doi.org/10.1029/2005GL024413>
- 1162 Tank, S. E., Frey, K. E., Striegl, R. G., Raymond, P. A., Holmes, R. M., McClelland, J. W., &  
1163 Peterson, B. J. (2012). Landscape-level controls on dissolved carbon flux from diverse  
1164 catchments of the circumboreal. *GLOBAL BIOGEOCHEMICAL CYCLES*, 26.  
1165 <https://doi.org/10.1029/2012GB004299>
- 1166 Tanski, G., Wagner, D., Knoblauch, C., Fritz, M., Sachs, T., & Lantuit, H. (2019). Rapid CO<sub>2</sub>  
1167 Release From Eroding Permafrost in Seawater. *Geophysical Research Letters*, 46(20).  
1168 <https://doi.org/10.1029/2019GL084303>
- 1169 Tanski, George, Bröder, L., Wagner, D., Knoblauch, C., Lantuit, H., Beer, C., ... Vonk, J. E.  
1170 (2021). Permafrost Carbon and CO<sub>2</sub> Pathways Differ at Contrasting Coastal Erosion Sites  
1171 in the Canadian Arctic. *Frontiers in Earth Science*, 9.  
1172 <https://doi.org/10.3389/feart.2021.630493>
- 1173 Tfaily, M. M., Hamdan, R., Corbett, J. E., Chanton, J. P., Glaser, P. H., & Cooper, W. T. (2013).  
1174 Investigating dissolved organic matter decomposition in northern peatlands using  
1175 complimentary analytical techniques. *Geochimica et Cosmochimica Acta*.  
1176 <https://doi.org/10.1016/j.gca.2013.03.002>
- 1177 Thurman, E. M. (1985). Organic geochemistry of natural waters (Vol. 2). Springer Science &  
1178 Business Media.



- 1179 Treat, C. C., Jones, M. C., Camill, P., Gallego-Sala, A., Garneau, M., Harden, J. W., ...  
1180 Väiliranta, M. (2016). Effects of permafrost aggradation on peat properties as determined  
1181 from a pan-Arctic synthesis of plant macrofossils. *Journal of Geophysical Research:*  
1182 *Biogeosciences*, 121(1), 78–94. <https://doi.org/10.1002/2015JG003061>
- 1183 Treat, Claire C., & Jones, M. C. (2018). Near-surface permafrost aggradation in Northern  
1184 Hemisphere peatlands shows regional and global trends during the past 6000 years.  
1185 *Holocene*. <https://doi.org/10.1177/0959683617752858>
- 1186 Turetsky, M. R., Wieder, R. K., Vitt, D. H., Evans, R. J., & Scott, K. D. (2007). The  
1187 disappearance of relict permafrost in boreal north America: Effects on peatland carbon  
1188 storage and fluxes. *Global Change Biology*, 13(9), 1922–1934.  
1189 <https://doi.org/10.1111/j.1365-2486.2007.01381.x>
- 1190 Turetsky, Merritt R., Abbott, B. W., Jones, M. C., Anthony, K. W., Olefeldt, D., Schuur, E. A.  
1191 G., ... McGuire, A. D. (2020). Carbon release through abrupt permafrost thaw. *Nature*  
1192 *Geoscience*. <https://doi.org/10.1038/s41561-019-0526-0>
- 1193 USDA. (1999). *Soil Taxonomy: A Basic System of Soil Classification for Making and*  
1194 *Interpreting Soil Surveys, 2nd Edition. Landscape and Land Capacity.*
- 1195 Varner, R. K., Crill, P. M., Frohling, S., McCalley, C. K., Burke, S. A., Chanton, J. P., ... Palace,  
1196 M. W. (2022). Permafrost thaw driven changes in hydrology and vegetation cover increase  
1197 trace gas emissions and climate forcing in Stordalen Mire from 1970 to 2014. *Philosophical*  
1198 *Transactions of the Royal Society A: Mathematical, Physical and Engineering Sciences*,  
1199 380(2215). <https://doi.org/10.1098/rsta.2021.0022>
- 1200 Vonk, J E, Tank, S. E., Mann, P. J., Spencer, R. G. M., Treat, C. C., Striegl, R. G., ... Wickland,  
1201 K. P. (2015). Biodegradability of dissolved organic carbon in permafrost soils and aquatic  
1202 systems: a meta-analysis. *BIOGEOSCIENCES*, 12(23), 6915–6930.  
1203 <https://doi.org/10.5194/bg-12-6915-2015>
- 1204 Vonk, Jorien E., & Gustafsson, Ö. (2013). Permafrost-carbon complexities. *Nature Geoscience*.  
1205 <https://doi.org/10.1038/ngeo1937>
- 1206 Weishaar, J. L., Aiken, G. R., Bergamaschi, B. A., Fram, M. S., Fujii, R., & Mopper, K. (2003).  
1207 Evaluation of specific ultraviolet absorbance as an indicator of the chemical composition  
1208 and reactivity of dissolved organic carbon. *Environmental Science and Technology*, 37(20),  
1209 4702–4708. <https://doi.org/10.1021/es030360x>
- 1210 Weyhenmeyer, G. A., Fröberg, M., Karlton, E., Khalili, M., Kothawala, D., Temnerud, J., &  
1211 Tranvik, L. J. (2012). Selective decay of terrestrial organic carbon during transport from  
1212 land to sea. *Global Change Biology*, 18(1). [https://doi.org/10.1111/j.1365-](https://doi.org/10.1111/j.1365-2486.2011.02544.x)  
1213 [2486.2011.02544.x](https://doi.org/10.1111/j.1365-2486.2011.02544.x)
- 1214 Wickland, K.P., Neff, J. C., & Aiken, G. R. (2007). Dissolved organic carbon in Alaskan boreal



- 1215 forest: Sources, chemical characteristics, and biodegradability. *Ecosystems*, 10(8), 1323–  
1216 1340. <https://doi.org/10.1007/s10021-007-9101-4>
- 1217 Wickland, Kimberly P, Waldrop, M. P., Aiken, G. R., Koch, J. C., Jorgenson, Mt., & Striegl, R.  
1218 G. (2018). Dissolved organic carbon and nitrogen release from boreal Holocene permafrost  
1219 and seasonally frozen soils of Alaska. *ENVIRONMENTAL RESEARCH LETTERS*, 13(6).  
1220 <https://doi.org/10.1088/1748-9326/aac4ad>
- 1221 Wild, B., Andersson, A., Broder, L., Vonk, J., Hugelius, G., McClelland, J. W., ... Gustafsson,  
1222 O. (2019). Rivers across the Siberian Arctic unearth the patterns of carbon release from  
1223 thawing permafrost. *PROCEEDINGS OF THE NATIONAL ACADEMY OF SCIENCES OF*  
1224 *THE UNITED STATES OF AMERICA*, 116(21), 10280–10285.  
1225 <https://doi.org/10.1073/pnas.1811797116>
- 1226 Wild, B., Gentsch, N., Capek, P., Diáková, K., Alves, R. J. E., Bárta, J., ... Richter, A. (2016).  
1227 Plant-derived compounds stimulate the decomposition of organic matter in arctic permafrost  
1228 soils. *Scientific Reports*, 6. <https://doi.org/10.1038/srep25607>
- 1229 Wild, B., Schnecker, J., Bárta, J., Čapek, P., Guggenberger, G., Hofhansl, F., ... Richter, A.  
1230 (2013). Nitrogen dynamics in Turbic Cryosols from Siberia and Greenland. *Soil Biology*  
1231 *and Biochemistry*, 67, 85–93. <https://doi.org/https://doi.org/10.1016/j.soilbio.2013.08.004>
- 1232 Woo, M. (1986). Permafrost hydrology in north america. *Atmosphere - Ocean*, 24(3).  
1233 <https://doi.org/10.1080/07055900.1986.9649248>
- 1234
- 1235
- 1236
- 1237
- 1238
- 1239
- 1240
- 1241
- 1242 **Studies used to generate database**
- 1243 Abbott, B. W., Jones, J. B., Godsey, S. E., Larouche, J. R., & Bowden, W. B. (2015). Patterns  
1244 and persistence of hydrologic carbon and nutrient export from collapsing upland permafrost.  
1245 *Biogeosciences*, 12(12), 3725–3740. <https://doi.org/10.5194/bg-12-3725-2015>



- 1246 Abbott, B. W., Larouche, J. R., Jones, J. J. B., Bowden, W. B., & Balsler, A. W. (2014). From  
1247 Thawing and Collapsing Permafrost. *Journal of Geophysical Research: Biogeosciences*,  
1248 119, 2049–2063. <https://doi.org/10.1002/2014JG002678>.Received
- 1249 Beckebanze, L., Runkle, B. R. K., Walz, J., Wille, C., Holl, D., Helbig, M., ... Kutzbach, L.  
1250 (2022). Lateral carbon export has low impact on the net ecosystem carbon balance of a  
1251 polygonal tundra catchment. *BIOGEOSCIENCES*, 19(16), 3863–3876.  
1252 <https://doi.org/10.5194/bg-19-3863-2022>
- 1253 Boddy, E., Roberts, P., Hill, P. W., Farrar, J., & Jones, D. L. (2008). Turnover of low molecular  
1254 weight dissolved organic C (DOC) and microbial C exhibit different temperature  
1255 sensitivities in Arctic tundra soils. *SOIL BIOLOGY & BIOCHEMISTRY*, 40(7), 1557–1566.  
1256 <https://doi.org/10.1016/j.soilbio.2008.01.030>
- 1257 Bristol, E. M., Connolly, C. T., Lorensen, T. D., Richmond, B. M., Ilgen, A. G., Choens, R. C.,  
1258 ... McClelland, J. W. (2021). Geochemistry of Coastal Permafrost and Erosion-Driven  
1259 Organic Matter Fluxes to the Beaufort Sea Near Drew Point, Alaska. *Frontiers in Earth  
1260 Science*, 8. <https://doi.org/10.3389/feart.2020.598933>
- 1261 Bruhn, A. D., Stedmon, C. A., Comte, J., Matsuoka, A., Speetjens, N. J., Tanski, G., ... Sjöstedt,  
1262 J. (2021). Terrestrial Dissolved Organic Matter Mobilized From Eroding Permafrost  
1263 Controls Microbial Community Composition and Growth in Arctic Coastal Zones.  
1264 *Frontiers in Earth Science*, 9. <https://doi.org/10.3389/feart.2021.640580>
- 1265 Buckeridge, K. M., & Grogan, P. (2008). Deepened snow alters soil microbial nutrient  
1266 limitations in arctic birch hummock tundra. *Applied Soil Ecology*, 39(2), 210–222.  
1267 <https://doi.org/https://doi.org/10.1016/j.apsoil.2007.12.010>
- 1268 Burd, K., Estop-Aragonés, C., Tank, S. E., & Olefeldt, D. (2020). Lability of dissolved organic  
1269 carbon from boreal peatlands: interactions between permafrost thaw, wildfire, and season.  
1270 *Canadian Journal of Soil Science*, 13(February), 1–13. <https://doi.org/10.1139/cjss-2019-0154>  
1271
- 1272 Burd, K., Tank, S. E., Dion, N., Quinton, W. L., Spence, C., Tanentzap, A. J., & Olefeldt, D.  
1273 (2018). Seasonal shifts in export of DOC and nutrients from burned and unburned peatland-  
1274 rich catchments, Northwest Territories, Canada. *Hydrology and Earth System Sciences*,  
1275 4455–4472. <https://doi.org/10.5194/hess-22-4455-2018>
- 1276 Carey, S. K. (2003). Dissolved organic carbon fluxes in a discontinuous permafrost subarctic  
1277 alpine catchment. *PERMAFROST AND PERIGLACIAL PROCESSES*, 14(2), 161–171.  
1278 <https://doi.org/10.1002/ppp.444>
- 1279 Chiasson-Poirier, G., Franssen, J., Lafreniere, M. J., Fortier, D., & Lamoureux, S. F. (2020).  
1280 Seasona evolution of active layer thaw depth and hillslope-stream connectivity in a  
1281 permafrost watershed. *WATER RESOURCES RESEARCH*, 56(1).  
1282 <https://doi.org/10.1029/2019WR025828>



- 1283 Connolly, C. T., Cardenas, M. B., Burkart, G. A., Spencer, R. G. M., & McClelland, J. W.  
1284 (2020). Groundwater as a major source of dissolved organic matter to Arctic coastal waters.  
1285 *NATURE COMMUNICATIONS*, 11(1). <https://doi.org/10.1038/s41467-020-15250-8>
- 1286 Cory, R. M., Crump, B. C., Dobkowski, J. A., & Kling, G. W. (2013). Surface exposure to  
1287 sunlight stimulates CO<sub>2</sub> release from permafrost soil carbon in the Arctic. *Proceedings of*  
1288 *the National Academy of Sciences*, 110(9), 3429–3434.  
1289 <https://doi.org/10.1073/pnas.1214104110>
- 1290 Deshpande, B. N., Crevecoeur, S., Matveev, A., & Vincent, W. F. (2016). Bacterial production  
1291 in subarctic peatland lakes enriched by thawing permafrost. *BIOGEOSCIENCES*, 13(15),  
1292 4411–4427. <https://doi.org/10.5194/bg-13-4411-2016>
- 1293 Douglas, T. A., Fortier, D., Shur, Y. L., Kanevskiy, M. Z., Guo, L., Cai, Y., & Bray, M. T.  
1294 (2011). Biogeochemical and Geocryological Characteristics of Wedge and Thermokarst-  
1295 Cave Ice in the CRREL Permafrost Tunnel, Alaska. *PERMAFROST AND PERIGLACIAL*  
1296 *PROCESSES*, 22(2), 120–128. <https://doi.org/10.1002/ppp.709>
- 1297 Drake, T. W., Wickland, K. P., Spencer, R. G. M., McKnight, D. M., & Striegl, R. G. (2015).  
1298 Ancient low-molecular-weight organic acids in permafrost fuel rapid carbon dioxide  
1299 production upon thaw. *PROCEEDINGS OF THE NATIONAL ACADEMY OF SCIENCES*  
1300 *OF THE UNITED STATES OF AMERICA*, 112(45), 13946–13951.  
1301 <https://doi.org/10.1073/pnas.1511705112>
- 1302 Dutta, K., Schuur, E. A. G., Neff, J. C., & Zimov, S. A. (2006). Potential carbon release from  
1303 permafrost soils of Northeastern Siberia. *GLOBAL CHANGE BIOLOGY*, 12(12), 2336–  
1304 2351. <https://doi.org/10.1111/j.1365-2486.2006.01259.x>
- 1305 Edwards, K. A., & Jefferies, R. L. (2013). Inter-annual and seasonal dynamics of soil microbial  
1306 biomass and nutrients in wet and dry low-Arctic sedge meadows. *Soil Biology and*  
1307 *Biochemistry*, 57, 83–90. <https://doi.org/https://doi.org/10.1016/j.soilbio.2012.07.018>
- 1308 Edwards, K. A., McCulloch, J., Kershaw, G. [Peter, & Jefferies, R. L. (2006). Soil microbial  
1309 and nutrient dynamics in a wet Arctic sedge meadow in late winter and early spring. *Soil*  
1310 *Biology and Biochemistry*, 38(9), 2843–2851.  
1311 <https://doi.org/https://doi.org/10.1016/j.soilbio.2006.04.042>
- 1312 Ernakovich, J. G., Lynch, L. M., Brewer, P. E., Calderon, F. J., & Wallenstein, M. D. (2017).  
1313 Redox and temperature-sensitive changes in microbial communities and soil chemistry  
1314 dictate greenhouse gas loss from thawed permafrost. *BIOGEOCHEMISTRY*, 134(1–2),  
1315 183–200. <https://doi.org/10.1007/s10533-017-0354-5>
- 1316 Ewing, S. A., Paces, J. B., O'Donnell, J. A., Jorgenson, M. T., Kanevskiy, M. Z., Aiken, G. R.,  
1317 ... Striegl, R. (2015). Uranium isotopes and dissolved organic carbon in loess permafrost:  
1318 Modeling the age of ancient ice. *GEOCHIMICA ET COSMOCHIMICA ACTA*, 152, 143–  
1319 165. <https://doi.org/10.1016/j.gca.2014.11.008>



- 1320 Fenger-Nielsen, R., Hollesen, J., Matthiesen, H., Andersen, E. A. S., Westergaard-Nielsen, A.,  
1321 Harmsen, H., ... Elberling, B. (2019). Footprints from the past: The influence of past human  
1322 activities on vegetation and soil across five archaeological sites in Greenland. *Science of the*  
1323 *Total Environment*, 654, 895–905. <https://doi.org/10.1016/j.scitotenv.2018.11.018>
- 1324 Fouché, J., Christiansen, C. T., Lafrenière, M. J., Grogan, P., & Lamoureux, S. F. (2020).  
1325 Canadian permafrost stores large pools of ammonium and optically distinct  
1326 dissolved organic matter. *Nature Communications*, 11(1), 4500.  
1327 <https://doi.org/10.1038/s41467-020-18331-w>
- 1328 Fouche, J., Bouchez, C., Keller, C., Allard, M., & Ambrosi, J.-P. (2021). Seasonal cryogenic  
1329 processes control supra-permafrost pore water chemistry in two contrasting Cryosols.  
1330 *GEODERMA*, 401. <https://doi.org/10.1016/j.geoderma.2021.115302>
- 1331 Fouché, J., Keller, C., Allard, M., Ambrosi, J. P., Fouche, J., Keller, C., ... Ambrosi, J. P. (2014).  
1332 Increased CO<sub>2</sub> fluxes under warming tests and soil solution chemistry in Histic and Turbic  
1333 Cryosols, Salluit, Nunavik, Canada. *Soil Biology and Biochemistry*, 68, 185–199.  
1334 <https://doi.org/https://doi.org/10.1016/j.soilbio.2013.10.007>
- 1335 Fritz, M., Opel, T., Tanski, G., Herzsuh, U., Meyer, H., Eulenburg, A., & Lantuit, H. (2015).  
1336 Dissolved organic carbon (DOC) in Arctic ground ice. *CRYOSPHERE*, 9(2), 737–752.  
1337 <https://doi.org/10.5194/tc-9-737-2015>
- 1338 Gagné, K. R., Ewers, S. C., Murphy, C. J., Daanen, R., Walter Anthony, K., & Guerard, J. J.  
1339 (2020). Composition and photo-reactivity of organic matter from permafrost soils and  
1340 surface waters in interior Alaska. *Environmental Science: Processes and Impacts*, 22(7),  
1341 1525–1539. <https://doi.org/10.1039/d0em00097c>
- 1342 Gao, L., Zhou, Z., Reyes V, A., & Guo, L. (2018). Yields and Characterization of Dissolved  
1343 Organic Matter From Different Aged Soils in Northern Alaska. *JOURNAL OF*  
1344 *GEOPHYSICAL RESEARCH-BIOGEOSCIENCES*, 123(7), 2035–2052.  
1345 <https://doi.org/10.1029/2018JG004408>
- 1346 Herndon, E. M., Mann, B. F., Chowdhury, T. R., Yang, Z., Wullschleger, S. D., Graham, D., ...  
1347 Gu, B. (2015). Pathways of anaerobic organic matter decomposition in tundra soils from  
1348 Barrow, Alaska. *JOURNAL OF GEOPHYSICAL RESEARCH-BIOGEOSCIENCES*,  
1349 120(11), 2345–2359. <https://doi.org/10.1002/2015JG003147>
- 1350 Herndon, E. M., Yang, Z., Bargar, J., Janot, N., Regier, T. Z., Graham, D. E., ... Liang, L.  
1351 (2015). Geochemical drivers of organic matter decomposition in arctic tundra soils.  
1352 *BIOGEOCHEMISTRY*, 126(3), 397–414. <https://doi.org/10.1007/s10533-015-0165-5>
- 1353 Herndon, E., AlBashaireh, A., Singer, D., Chowdhury, T. [Roy, Gu, B., & Graham, D. (2017).  
1354 Influence of iron redox cycling on organo-mineral associations in Arctic tundra soil.  
1355 *Geochimica et Cosmochimica Acta*, 207, 210–231.  
1356 <https://doi.org/https://doi.org/10.1016/j.gca.2017.02.034>



- 1357 Heslop, J. K., Chandra, S., Sobczak, W. V, Davydov, S. P., Davydova, A. I., Spektor, V. V, &  
1358 Anthony, K. M. W. (2017). Variable respiration rates of incubated permafrost soil extracts  
1359 from the Kolyma River lowlands, north-east Siberia. *POLAR RESEARCH*, 36.  
1360 <https://doi.org/10.1080/17518369.2017.1305157>
- 1361 Hirst, C., Mauclet, E., Monhonval, A., Tihon, E., Ledman, J., Schuur, E. A. G., & Opfergelt, S.  
1362 (2022). Seasonal Changes in Hydrology and Permafrost Degradation Control Mineral  
1363 Element-Bound DOC Transport From Permafrost Soils to Streams. *GLOBAL*  
1364 *BIOGEOCHEMICAL CYCLES*, 36(2). <https://doi.org/10.1029/2021GB007105>
- 1365 Hodgkins, S. B., Tfaily, M. M., Podgorski, D. C., McCalley, C. K., Saleska, S. R., Crill, P. M.,  
1366 ... Cooper, W. T. (2016). Elemental composition and optical properties reveal changes in  
1367 dissolved organic matter along a permafrost thaw chronosequence in a subarctic peatland.  
1368 *Geochimica et Cosmochimica Acta*, 187, 123–140.  
1369 <https://doi.org/10.1016/j.gca.2016.05.015>
- 1370 Jilkova, V., Devetter, M., Bryndova, M., Hajek, T., Kotas, P., Lulakova, P., ... Macek, P. (2021).  
1371 Carbon Sequestration Related to Soil Physical and Chemical Properties in the High Arctic.  
1372 *GLOBAL BIOGEOCHEMICAL CYCLES*, 35(9). <https://doi.org/10.1029/2020GB006877>
- 1373 Kane, E. S., Chivers, M. R., Turetsky, M. R., Treat, C. C., Petersen, D. G., Waldrop, M., ...  
1374 McGuire, A. D. (2013). Response of anaerobic carbon cycling to water table manipulation  
1375 in an Alaskan rich fen. *Soil Biology and Biochemistry*, 58, 50–60.  
1376 <https://doi.org/https://doi.org/10.1016/j.soilbio.2012.10.032>
- 1377 Kane, E. S., Valentine, D. W., Michaelson, G. J., Fox, J. D., & Ping, C.-L. (2006). Controls over  
1378 pathways of carbon efflux from soils along climate and black spruce productivity gradients  
1379 in interior Alaska. *Soil Biology and Biochemistry*, 38(6), 1438–1450.  
1380 <https://doi.org/https://doi.org/10.1016/j.soilbio.2005.11.004>
- 1381 Kane, E. S., Turetsky, M. R., Harden, J. W., McGuire, A. D., & Waddington, J. M. (2010).  
1382 Seasonal ice and hydrologic controls on dissolved organic carbon and nitrogen  
1383 concentrations in a boreal-rich fen. *JOURNAL OF GEOPHYSICAL RESEARCH-*  
1384 *BIOGEOSCIENCES*, 115. <https://doi.org/10.1029/2010JG001366>
- 1385 Kawahigashi, M., Prokushkin, A., & Sumida, H. (2011). Effect of fire on solute release from  
1386 organic horizons under larch forest in Central Siberian permafrost terrain. *Geoderma*,  
1387 166(1), 171–180. <https://doi.org/https://doi.org/10.1016/j.geoderma.2011.07.027>
- 1388 Koch, J. C., Runkel, R. L., Striegl, R., & McKnight, D. M. (2013). Hydrologic controls on the  
1389 transport and cycling of carbon and nitrogen in a boreal catchment underlain by continuous  
1390 permafrost. *JOURNAL OF GEOPHYSICAL RESEARCH-BIOGEOSCIENCES*, 118(2),  
1391 698–712. <https://doi.org/10.1002/jgrg.20058>
- 1392 Lim, A. G., Loiko, S. V, Kuzmina, D. M., Krickov, I. V, Shirokova, L. S., Kulizhsky, S. P., ...  
1393 Pokrovsky, O. S. (2021). Dispersed ground ice of permafrost peatlands: Potential



- 1394 unaccounted carbon, nutrient and metal sources. *Chemosphere*, 266, 128953.  
1395 <https://doi.org/10.1016/j.chemosphere.2020.128953>
- 1396 Lindborg, T., Rydberg, J., Tröjbom, M., Berglund, S., Johansson, E., Löfgren, A., ... Laudon, H.  
1397 (2016). Biogeochemical data from terrestrial and aquatic ecosystems in a periglacial  
1398 catchment, West Greenland. *Earth System Science Data*, 8(2), 439–459.  
1399 <https://doi.org/10.5194/essd-8-439-2016>
- 1400 Littlefair, C. A., & Tank, S. E. (2018). Biodegradability of Thermokarst Carbon in a Till-  
1401 Associated, Glacial Margin Landscape: The Case of the Peel Plateau, NWT, Canada.  
1402 *JOURNAL OF GEOPHYSICAL RESEARCH-BIOGEOSCIENCES*, 123(10), 3293–3307.  
1403 <https://doi.org/10.1029/2018JG004461>
- 1404 Liu, N., Michelsen, A., & Rinnan, R. (2020). Vegetation and soil responses to added carbon and  
1405 nutrients remain six years after discontinuation of long-term treatments. *Science of the Total  
1406 Environment*, 722, 137885. <https://doi.org/10.1016/j.scitotenv.2020.137885>
- 1407 Loiko, S. V, Pokrovsky, O. S., Raudina, T. V, Lim, A., Kolesnichenko, L. G., Shirokova, L. S.,  
1408 ... Kirpotin, S. N. (2017). Abrupt permafrost collapse enhances organic carbon, CO<sub>2</sub>,  
1409 nutrient and metal release into surface waters. *Chemical Geology*, 471, 153–165.  
1410 <https://doi.org/https://doi.org/10.1016/j.chemgeo.2017.10.002>
- 1411 MacDonald, E. N., Tank, S. E., Kokelj, S. V., Froese, D. G., & Hutchins, R. H. S. (2021).  
1412 Permafrost-derived dissolved organic matter composition varies across permafrost end-  
1413 members in the western Canadian Arctic. *Environmental Research Letters*, 16(2).  
1414 <https://doi.org/10.1088/1748-9326/abd971>
- 1415 Mangal, V., DeGasparro, S., Beresford, D. V, & Guéguen, C. (2020). Linking molecular and  
1416 optical properties of dissolved organic matter across a soil-water interface on Akimiski  
1417 Island (Nunavut, Canada). *Science of The Total Environment*, 704, 135415.  
1418 <https://doi.org/https://doi.org/10.1016/j.scitotenv.2019.135415>
- 1419 Masyagina, O. V, Tokareva, I. V, & Prokushkin, A. S. (2016). Post fire organic matter  
1420 biodegradation in permafrost soils: Case study after experimental heating of mineral  
1421 horizons. *Science of The Total Environment*, 573, 1255–1264.  
1422 <https://doi.org/https://doi.org/10.1016/j.scitotenv.2016.04.195>
- 1423 McFarlane, K. J., Throckmorton, H. M., Heikoop, J. M., Newman, B. D., Hedgpeth, A. L.,  
1424 Repasch, M. N., ... Wilson, C. J. (2022). Age and chemistry of dissolved organic carbon  
1425 reveal enhanced leaching of ancient labile carbon at the permafrost thaw zone.  
1426 *BIOGEOSCIENCES*, 19(4), 1211–1223. <https://doi.org/10.5194/bg-19-1211-2022>
- 1427 Mörsdorf, M. A., Baggesen, N. S., Yoccoz, N. G., Michelsen, A., Elberling, B., Ambus, P. L., &  
1428 Cooper, E. J. (2019). Deepened winter snow significantly influences the availability and  
1429 forms of nitrogen taken up by plants in High Arctic tundra. *Soil Biology and Biochemistry*,  
1430 135, 222–234. <https://doi.org/https://doi.org/10.1016/j.soilbio.2019.05.009>



- 1431 Neff, J. C., & Hooper, D. U. (2002). Vegetation and climate controls on potential CO<sub>2</sub>, DOC and  
1432 DON production in northern latitude soils. *Global Change Biology*, 8(9), 872–884.  
1433 <https://doi.org/10.1046/j.1365-2486.2002.00517.x>
- 1434 Nielsen, C. S., Michelsen, A., Strobel, B. W., Wulff, K., Banyasz, I., & Elberling, B. (2017).  
1435 Correlations between substrate availability, dissolved CH<sub>4</sub>, and CH<sub>4</sub> emissions in an arctic  
1436 wetland subject to warming and plant removal. *JOURNAL OF GEOPHYSICAL*  
1437 *RESEARCH-BIOGEOSCIENCES*, 122(3), 645–660. <https://doi.org/10.1002/2016JG003511>
- 1438 O'Donnell, J. A., Aiken, G. R., Butler, K. D., Guillemette, F., Podgorski, D. C., & Spencer, R.  
1439 G. M. (2016). DOM composition and transformation in boreal forest soils: The effects of  
1440 temperature and organic-horizon decomposition state. *JOURNAL OF GEOPHYSICAL*  
1441 *RESEARCH-BIOGEOSCIENCES*, 121(10), 2727–2744.  
1442 <https://doi.org/10.1002/2016JG003431>
- 1443 O'Donnell, J. A., Turetsky, M. R., Harden, J. W., Manies, K. L., Pruetz, L. E., Shetler, G., &  
1444 Neff, J. C. (2009). Interactive Effects of Fire, Soil Climate, and Moss on CO<sub>2</sub> Fluxes in  
1445 Black Spruce Ecosystems of Interior Alaska. *ECOSYSTEMS*, 12(1), 57–72.  
1446 <https://doi.org/10.1007/s10021-008-9206-4>
- 1447 Oiffer, L., & Siciliano, S. D. (2009). Methyl mercury production and loss in Arctic soil. *Science*  
1448 *of the Total Environment*, 407(5), 1691–1700.  
1449 <https://doi.org/10.1016/j.scitotenv.2008.10.025>
- 1450 Olefeldt, D., & Roulet, N. T. (2012). Effects of permafrost and hydrology on the composition  
1451 and transport of dissolved organic carbon in a subarctic peatland complex. *Journal of*  
1452 *Geophysical Research: Biogeosciences*, 117(1). <https://doi.org/10.1029/2011JG001819>
- 1453 Olefeldt, D., & Roulet, N. T. (2014). Permafrost conditions in peatlands regulate magnitude,  
1454 timing, and chemical composition of catchment dissolved organic carbon export. *Global*  
1455 *Change Biology*, 20(10), 3122–3136. <https://doi.org/10.1111/gcb.12607>
- 1456 Olefeldt, D., Roulet, N. T., Bergeron, O., Crill, P., Bäckstrand, K., & Christensen, T. R. (2012).  
1457 Net carbon accumulation of a high-latitude permafrost palsa mire similar to permafrost-free  
1458 peatlands. *Geophysical Research Letters*. <https://doi.org/10.1029/2011GL050355>
- 1459 Olsrud, M., & Christensen, T. R. (2011). Carbon partitioning in a wet and a semiwet subarctic  
1460 mire ecosystem based on in situ <sup>14</sup>C pulse-labelling. *Soil Biology and Biochemistry*, 43(2),  
1461 231–239. <https://doi.org/10.1016/j.soilbio.2010.09.034>
- 1462 Pastor, A., Poblador, S., Skovsholt, L. J., & Riis, T. (2020). Microbial carbon and nitrogen  
1463 processes in high-Arctic riparian soils. *PERMAFROST AND PERIGLACIAL PROCESSES*,  
1464 31(1), 223–236. <https://doi.org/10.1002/ppp.2039>
- 1465 Patzner, M. S., Mueller, C. W., Malusova, M., Baur, M., Nikeleit, V., Scholten, T., ... Bryce, C.  
1466 (2020). Iron mineral dissolution releases iron and associated organic carbon during



- 1467 permafrost thaw. *Nature Communications*, 11(1), 1–11. [https://doi.org/10.1038/s41467-020-](https://doi.org/10.1038/s41467-020-20102-6)  
1468 20102-6
- 1469 Patzner, M. S., Logan, M., McKenna, A. M., Young, R. B., Zhou, Z., Joss, H., ... Bryce, C.  
1470 (2022). Microbial iron cycling during palsa hillslope collapse promotes greenhouse gas  
1471 emissions before complete permafrost thaw. *Communications Earth & Environment*, 3(1),  
1472 76. <https://doi.org/10.1038/s43247-022-00407-8>
- 1473 Payandi-Rolland, D., Shirokova, L. S., Tesfa, M., Bénézeth, P., Lim, A. G., Kuzmina, D., ...  
1474 Pokrovsky, O. S. (2020). Dissolved organic matter biodegradation along a hydrological  
1475 continuum in permafrost peatlands. *Science of The Total Environment*, 749, 141463.  
1476 <https://doi.org/10.1016/J.SCITOTENV.2020.141463>
- 1477 Payandi-Rolland, D., Shirokova, L. S., Labonne, F., Bénézeth, P., & Pokrovsky, O. S. (2021).  
1478 Impact of freeze-thaw cycles on organic carbon and metals in waters of  
1479 permafrost peatlands. *Chemosphere*, 279, 130510.  
1480 <https://doi.org/10.1016/j.chemosphere.2021.130510>
- 1481 Payandi-Rolland, D., Shirokova, L. S., Nakhle, P., Tesfa, M., Abdou, A., Causserand, C., ...  
1482 Pokrovsky, O. S. (2020). Aerobic release and biodegradation of dissolved organic matter  
1483 from frozen peat: Effects of temperature and heterotrophic bacteria. *CHEMICAL*  
1484 *GEOLOGY*, 536. <https://doi.org/10.1016/j.chemgeo.2019.119448>
- 1485 Petersen, D. G., Blazewicz, S. J., Firestone, M., Herman, D. J., Turetsky, M., & Waldrop, M.  
1486 (2012). Abundance of microbial genes associated with nitrogen cycling as indices of  
1487 biogeochemical process rates across a vegetation gradient in Alaska. *Environmental*  
1488 *Microbiology*, 14(4), 993–1008. <https://doi.org/10.1111/j.1462-2920.2011.02679.x>
- 1489 Pokrovsky, O. S., Reynolds, B. C., Prokushkin, A. S., Schott, J., & Viers, J. (2013). Silicon  
1490 isotope variations in Central Siberian rivers during basalt weathering in permafrost-  
1491 dominated larch forests. *Chemical Geology*, 355, 103–116.  
1492 <https://doi.org/https://doi.org/10.1016/j.chemgeo.2013.07.016>
- 1493 Pokrovsky, O. S., Schott, J., Kudryavtzev, D. I., & Dupré, B. (2005). Basalt weathering in  
1494 Central Siberia under permafrost conditions. *Geochimica et Cosmochimica Acta*, 69(24),  
1495 5659–5680. <https://doi.org/10.1016/j.gca.2005.07.018>
- 1496 Pokrovsky, O. S., Manasypov, R. M., Loiko, S. V., & Shirokova, L. S. (2016). Organic and  
1497 organo-mineral colloids in discontinuous permafrost zone. *Geochimica et Cosmochimica*  
1498 *Acta*, 188, 1–20. <https://doi.org/https://doi.org/10.1016/j.gca.2016.05.035>
- 1499 Poulin, B. A., Ryan, J. N., Tate, M. T., Krabbenhoft, D. P., Hines, M. E., Barkay, T., ... Aiken,  
1500 G. R. (2019). Geochemical Factors Controlling Dissolved Elemental Mercury and  
1501 Methylmercury Formation in Alaskan Wetlands of Varying Trophic Status. *Environmental*  
1502 *Science and Technology*, 53(11), 6203–6213. <https://doi.org/10.1021/acs.est.8b06041>



- 1503 Prokushkin, A. S., Gavrilenko, I. V., Abaimov, A. P., Prokushkin, S. G., & Samusenko, A. V.  
1504 (2006). Dissolved organic carbon in upland forested watersheds underlain by continuous  
1505 permafrost in Central Siberia. *Mitigation and Adaptation Strategies for Global Change*,  
1506 *11*(1), 223–240. <https://doi.org/10.1007/s11027-006-1022-6>
- 1507 Prokushkin, A. S., Gleixner, G., McDowell, W. H., Ruehlow, S., & Schulze, E.-D. (2007).  
1508 Source- and substrate-specific export of dissolved organic matter from permafrost-  
1509 dominated forested watershed in central Siberia. *GLOBAL BIOGEOCHEMICAL CYCLES*,  
1510 *21*(4). <https://doi.org/10.1029/2007GB002938>
- 1511 Prokushkin, A. S., Kajimoto, T., Prokushkin, S. G., McDowell, W. H., Abaimov, A. P., &  
1512 Matsuura, Y. (2005). Climatic factors influencing fluxes of dissolved organic carbon from  
1513 the forest floor in a continuous-permafrost Siberian watershed. *CANADIAN JOURNAL OF*  
1514 *FOREST RESEARCH*, *35*(9), 2130–2140. <https://doi.org/10.1139/X05-150>
- 1515 Rasmussen, L. H., Michelsen, A., Ladegaard-Pedersen, P., Nielsen, C. S., & Elberling, B.  
1516 (2020). Arctic soil water chemistry in dry and wet tundra subject to snow addition, summer  
1517 warming and herbivory simulation. *Soil Biology and Biochemistry*, *141*, 107676.  
1518 <https://doi.org/https://doi.org/10.1016/j.soilbio.2019.107676>
- 1519 Raudina, T. V., Loiko, S. V., Lim, A., Manasyrov, R. M., Shirokova, L. S., Istigechev, G. I., ...  
1520 Pokrovsky, O. S. (2018). Permafrost thaw and climate warming may decrease the CO<sub>2</sub>,  
1521 carbon, and metal concentration in peat soil waters of the Western Siberia Lowland. *Science*  
1522 *of The Total Environment*, *634*, 1004–1023.  
1523 <https://doi.org/https://doi.org/10.1016/j.scitotenv.2018.04.059>
- 1524 Raudina, T. V., Loiko, S. V., Lim, A. G., Krickov, I. V., Shirokova, L. S., Istigechev, G. I., ...  
1525 Pokrovsky, O. S. (2017). Dissolved organic carbon and major and trace elements in peat  
1526 porewater of sporadic, discontinuous, and continuous permafrost zones of western Siberia.  
1527 *BIOGEOSCIENCES*, *14*(14), 3561–3584. <https://doi.org/10.5194/bg-14-3561-2017>
- 1528 Ro, H.-M., Ji, Y., & Lee, B. (2018). Interactive effect of soil moisture and temperature regimes  
1529 on the dynamics of soil organic carbon decomposition in a subarctic tundra soil.  
1530 *GEOSCIENCES JOURNAL*, *22*(1), 121–130. <https://doi.org/10.1007/s12303-017-0052-2>
- 1531 Roehm, C. L., Giesler, R., & Karlsson, J. (2009). Bioavailability of terrestrial organic carbon to  
1532 lake bacteria: The case of a degrading subarctic permafrost mire complex. *JOURNAL OF*  
1533 *GEOPHYSICAL RESEARCH-BIOGEOSCIENCES*, *114*.  
1534 <https://doi.org/10.1029/2008JG000863>
- 1535 Rogers, J. A., Galy, V., Kellerman, A. M., Chanton, J. P., Zimov, N., & Spencer, R. G. M.  
1536 (2021). Limited Presence of Permafrost Dissolved Organic Matter in the Kolyma River,  
1537 Siberia Revealed by Ramped Oxidation. *JOURNAL OF GEOPHYSICAL RESEARCH-*  
1538 *BIOGEOSCIENCES*, *126*(7). <https://doi.org/10.1029/2020JG005977>



- 1539 Roth, V.-N., Dittmar, T., Gaupp, R., & Gleixner, G. (2013). Latitude and pH driven trends in the  
1540 molecular composition of DOM across a north south transect along the Yenisei River.  
1541 *Geochimica et Cosmochimica Acta*, 123, 93–105.  
1542 <https://doi.org/https://doi.org/10.1016/j.gca.2013.09.002>
- 1543 Schostag, M., Stibal, M., Jacobsen, C. S., Baelum, J., Tas, N., Elberling, B., ... Prieme, A.  
1544 (2015). Distinct summer and winter bacterial communities in the active layer of Svalbard  
1545 permafrost revealed by DNA- and RNA-based analyses. *FRONTIERS IN*  
1546 *MICROBIOLOGY*, 6. <https://doi.org/10.3389/fmicb.2015.00399>
- 1547 Shakil, S., Tank, S. E., Kokelj, S. V., Vonk, J. E., & Zolkos, S. (2020). Particulate dominance of  
1548 organic carbon mobilization from thaw slumps on the Peel Plateau, NT: Quantification and  
1549 implications for stream systems and permafrost carbon release. *Environmental Research*  
1550 *Letters*, 15(11). <https://doi.org/10.1088/1748-9326/abac36>
- 1551 Shatilla, N. J., & Carey, S. K. (2019). Assessing inter-annual and seasonal patterns of DOC and  
1552 DOM quality across a complex alpine watershed underlain by discontinuous permafrost in  
1553 Yukon, Canada. *Hydrology and Earth System Sciences*, 23(9), 3571–3591.  
1554 <https://doi.org/10.5194/hess-23-3571-2019>
- 1555 Shirokova, L. S., Pokrovsky, O. S., Kirpotin, S. N., Desmukh, C., Pokrovsky, B. G., Audry, S.,  
1556 & Viers, J. (2013). Biogeochemistry of organic carbon, CO<sub>2</sub>, CH<sub>4</sub>, and trace elements in  
1557 thermokarst water bodies in discontinuous permafrost zones of Western Siberia.  
1558 *BIOGEOCHEMISTRY*, 113(1–3), 573–593. <https://doi.org/10.1007/s10533-012-9790-4>
- 1559 Shirokova, L. S., Bredoire, R., Rols, J.-L. L., & Pokrovsky, O. S. (2017). Moss and Peat  
1560 Leachate Degradability by Heterotrophic Bacteria: The Fate of Organic Carbon and Trace  
1561 Metals. *Geomicrobiology Journal*, 34(8), 641–655.  
1562 <https://doi.org/10.1080/01490451.2015.1111470>
- 1563 Shirokova, L. S., Chupakov, A. V., Zabelina, S. A., Neverova, N. V., Payandi-Rolland, D.,  
1564 Causserand, C., ... Pokrovsky, O. S. (2019). Humic surface waters of frozen peat bogs  
1565 (permafrost zone) are highly resistant to bio- and photodegradation. *BIOGEOSCIENCES*,  
1566 16(12), 2511–2526. <https://doi.org/10.5194/bg-16-2511-2019>
- 1567 Shirokova, L. S., Labouret, J., Gurge, M., Gerard, E., Ivanova, I. S., Zabelina, S. A., &  
1568 Pokrovsky, O. S. (2017). Impact of Cyanobacterial Associate and Heterotrophic Bacteria on  
1569 Dissolved Organic Carbon and Metal in Moss and Peat Leachate: Application to Permafrost  
1570 Thaw in Aquatic Environments. *AQUATIC GEOCHEMISTRY*, 23(5–6), 331–358.  
1571 <https://doi.org/10.1007/s10498-017-9325-7>
- 1572 Sistla, S. A., Schaeffer, S., & Schimel, J. P. (2019). Plant community regulates decomposer  
1573 response to freezing more strongly than the rate or extent of the freezing regime.  
1574 *ECOSPHERE*, 10(2). <https://doi.org/10.1002/ecs2.2608>



- 1575 Speetjens, N. J., Tanski, G., Martin, V., Wagner, J., Richter, A., Hugelius, G., ... Vonk, J. E.  
1576 (2022). Dissolved organic matter characterization in soils and streams in a small coastal  
1577 low-arctic catchment. *Biogeosciences*, 19(July), 3073–3097. Retrieved from  
1578 <https://doi.org/10.5194/bg-19-3073-2022>
- 1579 Stutter, M. I., & Billett, M. F. (2003). Biogeochemical controls on streamwater and soil solution  
1580 chemistry in a High Arctic environment. *Geoderma*, 113(1), 127–146.  
1581 [https://doi.org/https://doi.org/10.1016/S0016-7061\(02\)00335-X](https://doi.org/https://doi.org/10.1016/S0016-7061(02)00335-X)
- 1582 Takano, S., Yamashita, Y., Tei, S., Liang, M., Shingubara, R., Morozumi, T., ... Sugimoto, A.  
1583 (2021). Stable Water Isotope Assessment of Tundra Wetland Hydrology as a Potential  
1584 Source of Arctic Riverine Dissolved Organic Carbon in the Indigirka River Lowland,  
1585 Northeastern Siberia. *Frontiers in Earth Science*, 9.  
1586 <https://doi.org/10.3389/feart.2021.699365>
- 1587 Tanski, G., Couture, N., Lantuit, H., Eulenburg, A., & Fritz, M. (2016). Eroding permafrost  
1588 coasts release low amounts of dissolved organic carbon (DOC) from ground ice into the  
1589 nearshore zone of the Arctic Ocean. *Global Biogeochemical Cycles*, 30(7), 1054–1068.  
1590 <https://doi.org/10.1002/2015GB005337>
- 1591 Tanski, G., Lantuit, H., Ruttor, S., Knoblauch, C., Radosavljevic, B., Strauss, J., ... Fritz, M.  
1592 (2017). Transformation of terrestrial organic matter along thermokarst-affected permafrost  
1593 coasts in the Arctic. *Science of the Total Environment*, 581–582, 434–447.  
1594 <https://doi.org/10.1016/j.scitotenv.2016.12.152>
- 1595 Textor, S. R., Wickland, K. P., Podgorski, D. C., Johnston, S. E., & Spencer, R. G. M. (2019).  
1596 Dissolved Organic Carbon Turnover in Permafrost-Influenced Watersheds of Interior  
1597 Alaska: Molecular Insights and the Priming Effect. *FRONTIERS IN EARTH SCIENCE*, 7.  
1598 <https://doi.org/10.3389/feart.2019.00275>
- 1599 Thompson, M. S., Giesler, R., Karlsson, J., & Klaminder, J. (2015). Size and characteristics of  
1600 the DOC pool in near-surface subarctic mire permafrost as a potential source for nearby  
1601 freshwaters. *Arctic, Antarctic, and Alpine Research*, 47(1), 49–58.  
1602 <https://doi.org/10.1657/AAAR0014-010>
- 1603 Treat, C. C., Wollheim, W. M., Varner, R. K., & Bowden, W. B. (2016). Longer thaw seasons  
1604 increase nitrogen availability for leaching during fall in tundra soils. *ENVIRONMENTAL*  
1605 *RESEARCH LETTERS*, 11(6). <https://doi.org/10.1088/1748-9326/11/6/064013>
- 1606 Trusiak, A., Treibergs, L. A., Kling, G. W., & Cory, R. M. (2018). The role of iron and reactive  
1607 oxygen species in the production of CO<sub>2</sub> in arctic soil waters. *GEOCHIMICA ET*  
1608 *COSMOCHIMICA ACTA*, 224, 80–95. <https://doi.org/10.1016/j.gca.2017.12.022>
- 1609 Voigt, C., Lamprecht, R. E., Marushchak, M. E., Lind, S. E., Novakovskiy, A., Aurela, M., ...  
1610 Biasi, C. (2017). Warming of subarctic tundra increases emissions of all three important



- 1611 greenhouse gases – carbon dioxide, methane, and nitrous oxide. *Global Change Biology*,  
1612 23(8), 3121–3138. <https://doi.org/10.1111/gcb.13563>
- 1613 Voigt, C., Marushchak, M. E., Mastepanov, M., Lamprecht, R. E., Christensen, T. R.,  
1614 Dorodnikov, M., ... Biasi, C. (2019). Ecosystem carbon response of an Arctic peatland to  
1615 simulated permafrost thaw. *Global Change Biology*, 25(5), 1746–1764.  
1616 <https://doi.org/10.1111/gcb.14574>
- 1617 Voigt, C., Marushchak, M. E., Lamprecht, R. E., Jackowicz-Korczyński, M., Lindgren, A.,  
1618 Mastepanov, M., ... Biasi, C. (2017). Increased nitrous oxide emissions from Arctic  
1619 peatlands after permafrost thaw. *Proceedings of the National Academy of Sciences of the*  
1620 *United States of America*, 114(24), 6238–6243. Retrieved from  
1621 <https://www.jstor.org/stable/26484198>
- 1622 Vonk, J. E., Mann, P. J., Dowdy, K. L., Davydova, A., Davydov, S. P., Zimov, N., ... Holmes,  
1623 R. M. (2013). Dissolved organic carbon loss from Yedoma permafrost amplified by ice  
1624 wedge thaw. *ENVIRONMENTAL RESEARCH LETTERS*, 8(3).  
1625 <https://doi.org/10.1088/1748-9326/8/3/035023>
- 1626 Vonk, J. E., Mann, P. J., Davydov, S., Davydova, A., Spencer, R. G. M., Schade, J., ... Holmes,  
1627 R. M. (2013). High biolability of ancient permafrost carbon upon thaw. *GEOPHYSICAL*  
1628 *RESEARCH LETTERS*, 40(11), 2689–2693. <https://doi.org/10.1002/grl.50348>
- 1629 Waldrop, M. P., Harden, J. W., Turetsky, M. R., Petersen, D. G., McGuire, A. D., Briones, M. J.  
1630 I., ... Pruett, L. E. (2012). Bacterial and enchytraeid abundance accelerate soil carbon  
1631 turnover along a lowland vegetation gradient in interior Alaska. *Soil Biology and*  
1632 *Biochemistry*, 50, 188–198. <https://doi.org/https://doi.org/10.1016/j.soilbio.2012.02.032>
- 1633 Waldrop, M. P., & Harden, J. W. (2008). Interactive effects of wildfire and permafrost on  
1634 microbial communities and soil processes in an Alaskan black spruce forest. *GLOBAL*  
1635 *CHANGE BIOLOGY*, 14(11), 2591–2602. [https://doi.org/10.1111/j.1365-](https://doi.org/10.1111/j.1365-2486.2008.01661.x)  
1636 2486.2008.01661.x
- 1637 Ward, C. P., & Cory, R. M. (2015). Chemical composition of dissolved organic matter draining  
1638 permafrost soils. *Geochimica et Cosmochimica Acta*, 167, 63–79.  
1639 <https://doi.org/https://doi.org/10.1016/j.gca.2015.07.001>
- 1640 Ward, C. P., Nalven, S. G., Crump, B. C., Kling, G. W., & Cory, R. M. (2017). Photochemical  
1641 alteration of organic carbon draining permafrost soils shifts microbial metabolic pathways  
1642 and stimulates respiration. *NATURE COMMUNICATIONS*, 8.  
1643 <https://doi.org/10.1038/s41467-017-00759-2>
- 1644 Whittinghill, K. A., Finlay, J. C., & Hobbie, S. E. (2014). Bioavailability of dissolved organic  
1645 carbon across a hillslope chronosequence in the Kuparuk River region, Alaska. *Soil Biology*  
1646 *and Biochemistry*, 79, 25–33. <https://doi.org/https://doi.org/10.1016/j.soilbio.2014.08.020>



- 1647 Wickland, K. P., Neff, J. C., & Aiken, G. R. (2007). Dissolved organic carbon in Alaskan boreal  
1648 forest: Sources, chemical characteristics, and biodegradability. *ECOSYSTEMS*, 10(8),  
1649 1323–1340. <https://doi.org/10.1007/s10021-007-9101-4>
- 1650 Wickland, K. P., Waldrop, M. P., Aiken, G. R., Koch, J. C., Jorgenson, Mt., & Striegl, R. G.  
1651 (2018). Dissolved organic carbon and nitrogen release from boreal Holocene permafrost and  
1652 seasonally frozen soils of Alaska. *ENVIRONMENTAL RESEARCH LETTERS*, 13(6).  
1653 <https://doi.org/10.1088/1748-9326/aac4ad>
- 1654 Yun, J., Jung, J. Y., Kwon, M. J., Seo, J., Nam, S., Lee, Y. K., & Kang, H. (2022). Temporal  
1655 Variations Rather than Long-Term Warming Control Extracellular Enzyme Activities and  
1656 Microbial Community Structures in the High Arctic Soil. *MICROBIAL ECOLOGY*, 84(1),  
1657 168–181. <https://doi.org/10.1007/s00248-021-01859-9>
- 1658 Zolkos, S., & Tank, S. E. (2019). *Permafrost geochemistry and retrogressive thaw slump*  
1659 *morphology (Peel Plateau, Canada)*, v. 1.0 (2017-2017). [https://doi.org/10.5885/45573XD-](https://doi.org/10.5885/45573XD-28DD57D553F14BF0)  
1660 [28DD57D553F14BF0](https://doi.org/10.5885/45573XD-28DD57D553F14BF0)
- 1661